Miniaturized devices for DNA amplification and fluorescence based detection

Sudip Mondal AND V. Venkataraman

Abstract | MEMS technology has contributed substantially towards the development of Lab-on-a-Chip devices, whose aim is to replace bench-top laboratory tools with miniaturized chips for processing and detecting biomolecules. During the last decade there has been enormous amount of research towards finding the best material, simplifying fabrication techniques, improving biocompatibility and miniaturizing the device scale in order to deliver devices that are more efficient, cheaper, faster and have higher throughput. DNA based bio-chips must perform extraction of pure DNA from cell, amplification to detectable amounts and checking for product specificity. In this review we will discuss one of the important bio-MEMS applications, namely, DNA amplification devices using polymerase chain reaction (PCR). DNA amplification is used in various forms for pathogen detection, forensic investigations, bio-defence, food and water control, environmental monitoring, DNA sequencing etc. We will discuss the key aspects related to the miniaturization of PCR devices: material of choice, fabrication technologies, thermal measurement, feedback control and fluorescence based detection techniques.

Department of Physics, Indian Institute of Science, Bangalore 560 012, India
venki@physics.iisc.ernet.in

MEMS: Microelectromechanical systems (MEMS) are a class of devices ranging from micrometer to millimeter scale, incorporating mechanical, optical, chemical or biological functionality in addition to electronics. These devices are fabricated mostly by popular semiconductor manufacturing techniques. Most common MEMS material is silicon but recently many groups have started using hybrids of silicon with other materials such as glass and polymers.

Amplification: The process of increasing the number of copies of a given DNA fragment using polymerase chain reaction (PCR).

1. Introduction

The advancements in the field of MEMS technology has led to significant developments in miniaturized sensors and actuators. In the last decade, MEMS processing technology has been used to create miniaturized functional devices for applications in biology and medicine. Compared to bench-top machines, these devices can perform similar functions, but with smaller sample volumes, thus reducing time, cost and power consumption. Some of these devices are targeted for specific usage in the field of biomedical sample processing and analysis. Immense progress has been made in developing new materials that are bio-compatible and simpler for batch production. Various aspects of this progress has been discussed in recent reviews[1–4].

DNA amplification refers to the process of making multiple copies of a piece of DNA ("DNA xeroxing") using a technique known as Polymerase Chain Reaction (PCR). PCR for *in vitro* amplification of DNA was discovered by Kary Mullis in 1983[5]. Mullis received the Nobel Prize in 1993 for this landmark discovery. Since then it has been used successfully to amplify DNA from a variety of sources. PCR is an enzyme mediated method that is driven by temperature dependent DNA manipulation as shown in Figure 1. The PCR mix is a small volume of aqueous solution ($\sim$ few μL) containing a few copies of the DNA segment that has to be amplified ("template DNA"), a large concentration of primers (artificially synthesized ss-DNA, typically 15–30 bp long, specific to the

Figure 1: Schematic of DNA amplification by PCR. The colours denote the four different bases (A,T,C,G). Note that the two strands forming the double helix are complementary i.e. A pairs with T and C with G.

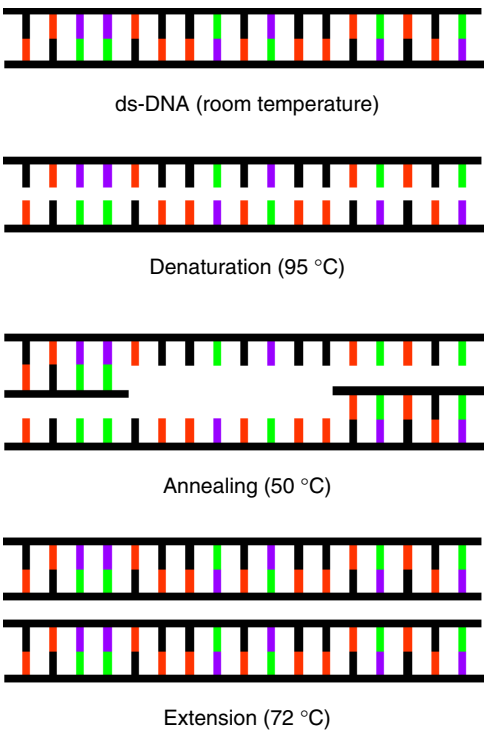

template), dNTPs (building blocks of the DNA strand), Taq Polymerase (an enzyme that catalyzes DNA polymerization), and other salts and buffers that maintain the pH of the mix. The manipulation steps involved are:

1. denaturation: the mix is heated to 95 °C so that all the hydrogen bonds, that stabilize the ds-DNA, break down to form two ss-DNA.
2. annealing: the mix is then cooled to ∼50 °C when the primers anneal to the denatured templates. A set of primers are designed to have specific binding locations in the two complementary template strands. The sequence of the primers decides the annealing temperature.
3. extension: the temperature of the mix is raised to 72 °C, specific to the thermostable DNA polymerase. During this step the DNA polymerase extends the primer annealed template to form two ds-DNA.

The above thermocycle steps are repeated for ∼35 cycles to produce large number of copies of a specific segment of the DNA. From Figure 1 it is clear that the amount of DNA doubles in every cycle and after n cycles we expect the amount to increase by 2^n. Hence a PCR can produce nearly millions of copies of a DNA fragment of interest starting from a single copy of template. With the production of such a large quantity of DNA it becomes relatively easy to detect the product without expensive equipment and reagents. More importantly, since amplification occurs only if the primers match a specific region of the template DNA, the presence or absence of amplified DNA can be used to distinguish different template DNA, even if they differ by a single base pair. This specificity is the key for the importance of PCR in a variety of applications such as mutation detection, DNA fingerprinting and medical diagnostics.

The cycling rate in bench-top thermocyclers is as follows. About 20–50 μL of the PCR solution is loaded in a polypropylene tube which is inserted into a metal block. Polypropylene is cheap and biocompatible, but has poor thermal conductivity. Therefore the metal block ensures thermal homogeneity and a means for accurate temperature monitoring. The metal block is attached to a high power active peltier unit for rapid heating and cooling. The huge thermal mass of the block makes the ramping slow and the cycler needs to ensure sufficient stay time at all the three temperatures for the thermal processes to occur. With typical heating and cooling rates of 2–5°C/s, the whole process of amplification requires ∼2 hours to complete. The amplified product is analyzed by gel electrophoresis for checking the product specificity which takes another ∼ 1–2 hours time. In order to shorten the cycling time, it can be noted that denaturation and annealing are instantaneous processes, so they will occur immediately once the correct temperature is reached in the solution. Extension being polymerase driven, will need finite time to complete depending on the efficiency of the polymerase, length of the DNA to be extended and temperature. Since a substantial fraction of the time is spent on ramping and reaching the homogeneous temperature, it is possible to reduce the total time of cycling by using a system with low thermal mass, high thermal conductivity and small solution volume. This has been achieved by utilizing MEMS technologies that can produce devices with very low thermal mass from silicon or other materials with good thermal properties. Smaller devices also have higher surface to volume ratio which improves the cooling rate and obviates the necessity to have active cooling devices such as peltier coolers or fans.

Miniaturized PCR devices can be broadly divided into stationary thermal chamber type and

DNA (ss-DNA and ds-DNA): Deoxyribonucleic acid (DNA) is the molecule which forms the genetic material of all living organisms. In animals and plants, it is an important component of chromosomes. Chemically, single strand DNA (ss-DNA) consists of a polynucleotide chain while double strand DNA (ds-DNA) consists of a pair of chains running in opposite directions to each other. Each chain in ds-DNA has a sugar-phosphate backbone. One of the four bases, adenine, cytosine, guanine and thymine is attached to each sugar in the backbone. These bases are joined by hydrogen bonds which are formed between adenine in one chain and the thymine in the other and between the cytosine in one chain and the guanine in the other. The whole ds-DNA molecule is twisted to form a double helix with one complete turn of the spiral for every ten base pairs.

Template: Template is the ds-DNA added to the PCR mixture, a segment of which will be amplified. The primers added to the mixture are complementary to a part of each of the template strands. The primer annealing sites on the template decide the size of the amplified product.

Thermostable DNA polymerase: DNA polymerase is an enzyme (a kind of protein molecule) that binds to a partially formed ss-DNA and extends it by incorporating complementary bases to form the complete ds-DNA. The present polymerase molecules are stable up to sufficiently high temperature to be used in PCR for 30–40 cycles.

Base pair: The primary building blocks of DNA are called bases namely, adenine (A), cytosine (C), guanine (G) and thymine (T). The number of these bases decides the length of the DNA. For example, if there are n bases stacked in each of the complementary strands to form a ds-DNA, it will be called as an n-base pair (bp) ds-DNA.

Electrophoresis: A charged particle in an electric field will experience Coulomb force and be dragged towards one of the electrodes. DNA being negatively charged in solution will experience a similar force and is attracted by the positive electrode. Depending on the size of the DNA, it will have different mobility and moves with different speed. In practice the DNA is moved under electric field inside an agarose gel matrix in order to separate framents of different sizes. This process is known as electrophoresis.

Capillary: Capillary is a narrow tube or channel through which fluid can flow through. The smallest capillary for blood circulation in the human body is about 5–10 micron in diameter. Artificial capillaries are fabricated using lithography techniques from silicon, glass, polymer etc. to flow fluids in bench top systems and microdevices.

Fluorophore: These are dye molecules that can be excited from ground state to higher states using photons. Some of these molecules return to ground state by emitting photons at higher wavelength, called fluorescence. The fluorophores are designed to have specific excitation and emission wavelengths. SYBR green I dye (SG) is one such molecule with excitation and emission peak at 488 and 520 nm respectively. SG is an intercalating dye and produces large fluorescence only when it is bound to ds-DNA compared to free molecules or bound to ss-DNA.

continuous flow type. In stationary devices a small chamber is filled with PCR solution and rapidly cycled through the three temperature steps as in a conventional cycler. However it should be noted that while conventional cyclers use peltier cooling, most microchip PCR devices use passive cooling or, in some cases, forced air cooling. This is sufficient to achieve reasonable cooling rates since the thermal mass is low and surface to volume ratio is high. In flow through PCR devices the sample solution is forced through a capillary across three static temperature zones repeatedly using pressure. Though flow-through type devices do not spend time in ramping between different temperatures, they require microfluidic pumps for adjusting the pressure to maintain the flow. In the remainder of this review, we focus attention only on stationary chamber type devices.

Once the DNA is amplified, it has to be measured and quantified. In practice amplified DNA is loaded in agarose or poly-acrylamide gel and electrophoresed for nearly 1-2 hours to check the product specificity. Products of different lengths will have different mobility in the gel producing well separated bands when they are moved in a strong electric field. Electrophoresis is an end point detection that does not give intra cycle information. Fluorescence techniques developed for PCR, generally called quantitative PCR (qPCR) or real-time PCR (RT-PCR) can provide detailed information related to reaction kinetics of the PCR. Fluorescence detection techniques can be sequence independent or sequence dependent. In the former, a sequence independent fluorophore gives fluorescence whenever it binds to ds-DNA while the other class of fluorophore works only with a known type of template. The fluorescence intensity from these fluorophores are recorded during PCR to provide information about the amplification.

Figure 2 shows the main components of a conventional cycling block compared to a microchip device. Benchtop thermal cyclers are capable of running many parallel reactions simultaneously at the expense of slow ramp rates due to the large thermal mass. The integrated heater and sensor produces uniform thermal profile using proportional-integral-differential (PID) control. In RT-PCR systems, each of the reactions can be monitored individually using fibre optics coupled to sensitive detectors. On the other hand, microchip PCR devices are fabricated on relatively thinner substrates of good thermal conductivity material such as silicon. These devices are small and produce high ramp rates with good thermal control.

Table 1 compares key performance parameters of a tabletop block thermocycler ("Conventional PCR") and the microchip devices ("Chip PCR"). From this table it is evident that the chip thermocycler is faster, consumes less power and requires smaller reaction volumes. In addition, arrays of microchip devices can be built where individual reactions can be independently controlled. Before realizing these advantages of miniaturization, one must however confront with some challenging problems. For instance, loading and recovery of small reaction volumes in the reservoir is an issue. The large surface to volume ratio of microchips leads to adverse surface reactions and large thermal gradients. Measuring and controlling the temperature of the reaction mix ("a tiny droplet of water") is a challenging task. Finally the mix has to be properly sealed at $\sim 95\,^{\circ}C$ (It is easy to lose this "drop of water" by evaporation !).

Table 1: Comparison of key parameters of conventional thermocycler and microchip PCR devices.

Property	Conventional	Chip
Sample Volume (μL)	20–50	3
Heating and cooling rate (°C/s)	2	$\geq$20
Heat block mass	$\sim$1 kg	$\sim$100 gm
Total analysis time (Hr)	2	$<$0.5
Power used (W/device)	20	2
Cost	high	low

We summarize in Table 2 some of the important components of microchip devices and issues relevant to them. Each of these issues will be discussed in detail in the following sections.

2. Evolution of microchip PCR

During the early days of its discovery, PCR was very difficult to practice since the DNA polymerase used was not stable at high temperatures and degraded at $95\,^{\circ}C$ which was required for denaturing the ds-DNA. The polymerase was replaced by a fresh amount after each high temperature treatment at denaturation step. The heat treatments were done using hot water baths in large volumes. Only after the development of heat stable DNA polymerase such as *Thermus aquaticus* or *Taq* the process could be completed without any interventions[6]. This development in the field of polymerase engineering led to the possibility of incorporating the technique first into benchtop automatic cyclers and later into small scale devices.

A rapid temperature cycler fabricated from glass capillary tubes with low thermal mass was first demonstrated by Wittwer et al. in 1990[7]. A silicon micro device for PCR was first demonstrated by Northrup et al. in 1993[8]. After this pioneering work, the field has grown exponentially during

PCR Mixture or solution: Amplification of DNA using PCR requires some basic components that form the PCR solution such as template, bases, DNA polymerase, $MgCl_2$, HCl, etc. Once they are added in correct proportion, amplification occurs by thermal cycling.

Figure 2: A commercial sample block (A) with integrated heater and sensor units in comparison to a typical microchip device (B). Note the difference in scale.

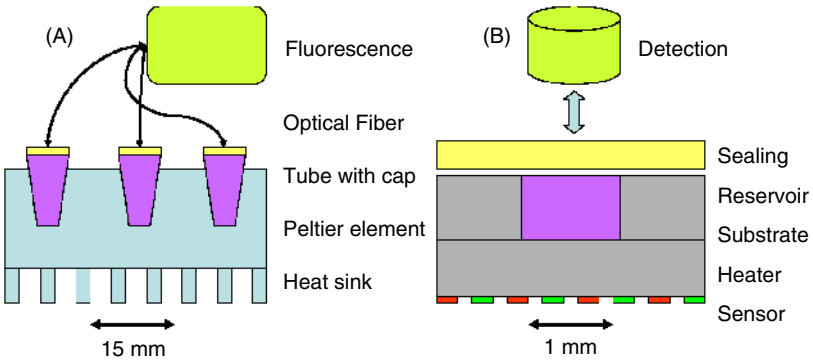

the last decade and today we have a large number of groups working in this area. In an attempt to optimize the thermal homogeneity in the solution, various PCR chamber designs such as droplet[9], well with vertical extension[10], well with uniform extension[11–20], spiral[21], channel[22] etc have been tested. PCR has been used to amplify DNA from very diverse samples, for example, blood[23], tissues[24], wastewater[25], and soil[26].

Extending the miniaturization concept to complete Lab-on-a-Chip (LOC) system is based on the fact that small integrated systems can perform operations faster and with greater functionality. Apart from PCR, development of product analysis is an important step. It is required to detect and analyze the nature of the product formed within a short time to be able to integrate it along with amplification on a LOC platform. In conventional protocols this is achieved by an elaborate and time consuming process of separating the DNA formed after PCR in agarose gel electrophoresis. Attempts have been made to develop real time detection techniques to analyze the product quickly and reproducibly on chip. There has been tremendous progress towards the integration of different components to make a complete LOC device. Figure 3 shows this trend for last 10 years till April 13th of 2007.

Table 2: Design issues involving the important components of a microchip PCR device.

Component	Choices	Issues
Substrate	material: Si, SiO_2, polymer	biocompatibility, thermal conductivity, optical characteristics
Reservoir	Size and shape	flat planar design for uniform temperature but increased adverse surface effects
Heater	material, shape, placement	least thermal coefficient, easy to fabricate, shape to produce uniform thermal profile
Sensor	material, shape, placement	high thermal coefficient, easy to fabricate, close to the reservoir
Sealing	material: tape, wax, oil	biocompatibility, seal at high temperature, optical properties
Detection	technique: end point, real time	miniaturizable, sensitivity, fast data acquisition

3. Material for microchip devices

Today there exist a number of materials that can be processed to form a bioanalysis device. Initial reports used well known materials such as silicon, silicon-dioxide and glass but lately attempts are being made to replace them by new materials which are comparatively physically soft, electrically insulating, optically transparent and cheap such as plastic, elastomer and polymer.

3.1. *Hard material for fabrication*

Thermal response of the microchip has been analyzed and studied in detail to understand the steady state and transient response. This helps in developing the microchip design with inbuilt heater and sensor. Most of the early devices were designed with silicon as a substrate having the micro reactor and a thick glass plate on the top to seal the solution from evaporation at high temperature. Since glass is a poor thermal conductor, most of the heat is dissipated through the substrate. Hence the thickness and the thermal mass of the base material is a critical component in the optimization of device performance. Silicon being a good thermal conductor can enhance the cooling rate for reduced thickness. Use of smaller dimension of micro reservoir can be of advantage in cutting down the power consumption.

Low background fluorescence from silicon substrates enables high sensitivity for fluorescence detection units. Most of the silicon micro devices are packaged with optically transparent glass material

Figure 3: Search results on PubMed for last 10 years. The number of publications were restricted to the english language and the words as mentioned in the legend.

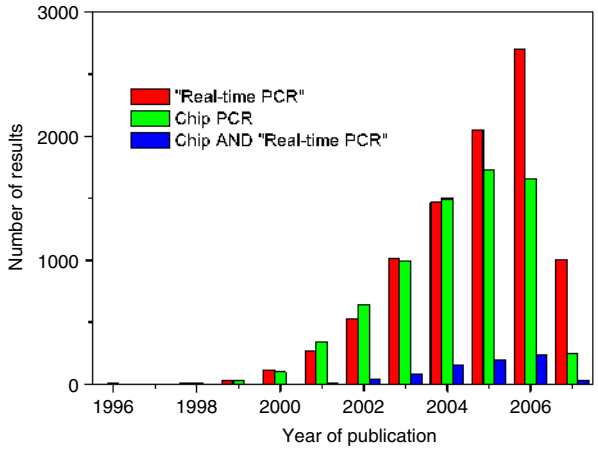

for thermal sealing and allow optical detection from top. Devices made from complete glass structures are useful for inverted optical microscopy studies.

Apart from using glass in microchambers for sealing, it has been used in the form of capillary tubes as reservoirs for PCR[7,27,28]. Some of the early capillary PCR was performed with comparatively higher volume (~10 μL) and by using hot air thermocycler. The thinner capillary (~150 μm inner diameter and ~375 μm outer diameter) primarily led to a significant reduction in reaction volume and consequently to enhanced thermal characteristics[28].

3.2. *Soft material as a replacement*

Soft material based micro reactors are increasingly being developed over the last few years in order to realize inexpensive and disposable miniaturized devices. Plastic and polymer are the best choice for this purpose because they have good material compatibility with bioreagents. These materials are also easy to mould into the shape of micro chambers with integrated heater and sensor components by multilayer bonding. However the thermal response of polymeric materials is slow due to their poor thermal conductivity.

Giordano et al.[29] used polyimide material for prototyping micro chambers for amplifying DNA. They used polyimide sheet of thickness 150 μm and used laser ablation to remove materials selectively from the sheet to get the shape for micro chamber and access hole for injection. Three layers with access hole, reservoir and an unpunched one were stacked together to form the micro PCR device. It was then cycled through temperatures using infrared radiation. A microfluidic PCR device capable of performing temporal and spatial cycling of sample volumes as small as 12 nL was demonstrated using an elastomer material polydimethylsiloxane (PDMS) by Liu et al.[30].

Polyethylene terephthalate (PET) plastic microchip fabricated from silicon mould by thermal forming was demonstrated by Zou et al.[14]. Silicon moulds with 400 μm cavities produced PET array devices with 20 μL chamber volume that were heated and cooled by placing the array on a PCB with individual heaters. SU-8 is a polymer extensively used in semiconductor industry. This polymer can easily be spin coated on any substrate to produce layers of large thickness such as ~200 μm. Ali et al.[16] used 400 μm SU-8 layer to fabricate a PCR chamber with in-built platinum heater and sensor that produced heating and cooling rates of 30 °C/s. A thin layer of SU-8 was used on the platinum electrode for protection and for bonding a glass cover on to the chip. The reservoir with SU-8 material on all sides was found to amplify DNA templates only with high concentration of DNA polymerase. Passivating the surface with a silanizing agent, dichlorodimethylsilane, showed successful PCR with normal polymerase concentration. Panaro et al. tested several plastics and commercially available plastic tubing for biocompatibility with respect to PCR[31]. Many reports have summarized important materials properties useful for PCR devices[2,12,17,32]. Some of them are listed in Table 3.

Table 3: Properties of microfabrication materials. Data compiled from[2,12,17,32,33]

Property	Silicon	SiO2	Pyrex	PDMS
Density (g/cm^3)	2.3	2.2	2.23	0.97×10^{-3}
Elasticity modulus (GPa)	165	73	63	$\sim 8 \times 10^{-4}$
Poisson ratio	0.22	0.17	0.2	0.5
Bulk resistivity (Ωcm)	2.3×10^5	$>10^4$	$>10^4$	$>10^{14}$
Dielectric constant	11.9	3.9	4.1	2.65
Heat capacity (J/g-°C)	0.7	1.0	0.75	1.46
Thermal cond. (W/cm-K)	1.5	0.014	0.011	0.0018
Max. process temp. (°C)	1415	1700	550–600	~150
Refractive index	3.49	1.46	1.47	1.4

4. Surface effects on PCR

With increase in surface to volume ratio in small scale devices it becomes important to study the surface properties with respect to the biological samples. Since the solution contains different kinds of ionic components that are cycled through high temperatures, surface modification agents need to be selected carefully. Earlier, devices were all fabricated from silicon which has affinity towards protein molecules. Later this material was replaced by alternatives such as silicon-dioxide and polymer that are relatively more biocompatible. Some groups

Photolithography: Photolithography is a process by which a pattern is transferred to a photo sensitive material (photoresist) coated on a substrate using UV light. The resist when exposed to light through a mask changes its properties. After developing in a suitable chemical, the pattern on the mask is transferred to the photoresist.

have modified the solution components in order to overcome the surface related issues. In an attempt towards understanding the adverse surface adsorption effects, many groups have exposed the untreated microchip walls to the essential components of the PCR for a specified time and then tested them for amplification efficiency. It has been found by most of the groups that exposing the chip surface to DNA or primers has very little effect on efficiency. DNA polymerase on the other hand, becomes inactive on incubation to most of the untreated chip surfaces and the PCR mix shows amplification only on addition of fresh polymerase keeping all other components the same. Some labs have used treated and untreated foreign particles within PCR solution in tubes to test their effect on efficiencies[34]. Oda et al.[35] found the inhibition of PCR due to presence of metal surfaces in the form of a thermocouple temperature sensor with outer diameter of 0.005 inch.

In an ideal bio-chip system, microreactors need to be disposable and do not need to be cleaned after a PCR run for reusing. But some laboratories have studied the effect of cleaning silicon microchips using acids and other reagents. Erill et al. have used a 8 mm tube peristaltic pump through a custom made cleaning arrangement to flow continuously and sequentially the washing reagents to the microchip[36]. Flushing was done for 5 min each with 37% hydrochloric acid ($HCl:H_2O_2:H_2O$ :: 1:1:5), 30% ammonia ($NH_3:H_2O_2:H_2O$ :: 1:1:5), 96% ethanol and 18.2 MΩ deionized water. After the treatment the chip was blow dried with N_2 flow and autoclaved at 2.2 bar-135 °C for 15 min.

Since surface effects for some designs are found to be significant, it is important to investigate methods for passivating the chips. In general there are two kind of passivation, static and dynamic.

4.1. *Static passivation*

In static passivation, the inner surface of the chip that is in contact with the PCR solution is coated with materials that are more biocompatible. Devices that are fabricated from silicon are oxidized at high temperature during the wafer processing steps to avoid silicon surface from coming in contact with the solution. Attempts were made to use silicon-nitride surfaces but did not prove to be successful[34]. Devices with glass have also proved to be biocompatible, and have been used by many groups to fabricate hybrid devices along with silicon technology. One other example of static passivation is pre-coating inner walls of the chip with different materials. Anderson et al.[37] coated the chamber of their microchip with parylene-C to get reproducible enzymatic performance. Coating the surfaces with silanizing agents such as SurfaSil^{TM} followed by polyadenylic acid or polyvinylpyrrolidone produces amplicons at same efficiency as those produced in polymer tubes[34]. A treatment of the microchip surface with silanizing agent such as hexamethyldisilazane (HMDS) prior to the PCR showed no effect of inhibition[38].

4.2. *Dynamic passivation*

In this kind of passivation external additives are added to the PCR solution to combat the adverse effect of surface adsorption to the microchip walls. Silicon microchips with lower efficiency to amplify DNA are shown to improve by adding carrier protein Bovine serum albumin (BSA) in the mix. Final concentration of 5 μg/μL was found to be optimum for the amplification, with higher concentrations reducing the yield probably due to increased mix viscosity leading to reduced mobility of the enzyme that limits enzyme activity[38–40]. Surfactant Tween 20 used in protein or nucleic acid handling reduces the surface tension of the solution and helps in dispersing, emulsifying and dissolving solution components to protect the enzyme. A final amount of 10% was found to be optimal to increase the efficiency to maximum[38]. Additives such as polyethylene glycol (PEG) in small amount ∼0.75% can enhance the PCR efficiency in microchip made of polymeric or plastic materials[29]. It has been found to improve the PCR compatibility properties of metals and maintain the efficiencies for reusability[31].

Apart from the above additives, it is advisable to increase the DNA polymerase amount in microchip PCR. Using very low concentration of polymerase increases the probability of surface adsorption and leaves out little free polymerase in the solution. Hence it is important that sufficient polymerase is available in the mix which is ensured when using titrated amount of BSA that balances the surface adsorption phenomena. Taylor et al.[39] studied varying concentration of polymerase in the mix and found that lower than 0.025 U/μL did not show any amplification. Most of the groups have been using 0.05-0.1 U/μL of DNA polymerase in silicon-glass devices[38–40]. Increase in the amount of polymerase also requires increased concentration of Mg^{2+} in the mix[39].

5. Fabrication techniques for PCR devices

The different fabrication methods reported for Bio-MEMS devices include standard semiconductor processing, soft lithography, hot embossing, injection molding, xurography etc. In this review we describe silicon processing and soft lithography. Semiconductor industry utilizes single crystal silicon wafers that are optically flat and have very

Figure 4: Soft lithography using PDMS elastomer and master mould.

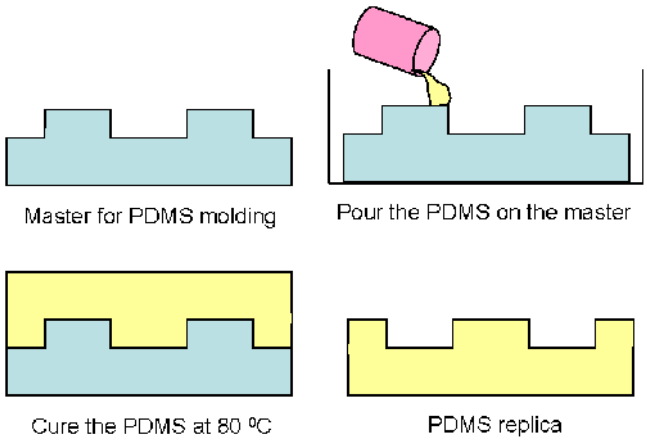

good thermal, electrical and mechanical properties. Silicon has been used by the integrated chip industry for a long time for CMOS technology. Silicon device fabrication technology has been so well optimized down to nm scale devices that it became an obvious material choice even for bio-MEMS devices. The processing steps to obtain silicon devices include photolithography, etching, metallization and bonding.

5.1. *Photolithography*

Photolithography is one of the most widely used techniques to transfer a pattern to the wafer[32]. A stencil containing the features that are to be transferred on the substrates is prepared on glass using a metal layer that will selectively allow UV radiation. The wafer on which the pattern needs to be transferred is cleaned and coated with a photosensitive resist using a spin coater. Depending on the spinner speed, time, wafer size, and resist viscosity, it is possible to get a uniformly coated thickness. The photoresist coated wafer is soft baked at ~90 °C to remove all solvents from the photoresist and increase its adhesion. Then it is exposed to UV light with sufficient intensity to polymerize the whole thickness of the photoresist through the openings in the stencil.

For positive resist, the exposed part is dissolved and removed by using a developer solution. If negative resist is used, it is the exposed part that remains while removing the unexposed resist material. The developed pattern is then hard baked at ~120 °C and the patterned substrate can either be etched or covered with metal film by lift off. For etching, the sample is immersed in a solution for wet etching or in a reactive ion plasma chamber for dry etching. This removes the material that is exposed to the solution or ions while other parts are protected by the resist mask. In practice, photoresist mask is first used on an oxidized substrate to etch the thin layer of silicon-dioxide layer using buffered hydro fluoric acid (BHF) solution. This pattern is then transfered to silicon using isotropic or anisotropic etching solution (for example KOH and TMAH at ~80 °C) to produce high aspect ratio structures. Depending on the orientation of the silicon wafers, different profiles are produced after etching[41,42]. The resist is then removed by using a suitable resist remover. In case of metal lift off, the patterned wafer is metallized using vacuum evaporation or sputtering so that a thin layer of metal gets coated uniformly all over the surface. The metal coated sample is then placed in resist remover solution to remove the resist along with the metal film on the top, leaving the metal on the bare substrate. These two techniques can be repeated many times using an aligner to obtain multilayer patterns.

5.2. *Soft lithography*

Though most of the early microfluidics were built on silicon-glass materials using standard semiconductor technology, recently many groups have developed alternative techniques using polymeric material to demonstrate similar ideas. The need for rapid prototyping requires simpler and versatile fabrication protocols that can be practiced in near-ambient environment unlike silicon technology. These requirements have led to the development of soft lithography using polymers, plastics, elastomers etc.[43–46]. Among the soft polymeric materials that has replaced silicon very successfully is polydimethylsiloxane (PDMS). PDMS comprises of repeating units of -O-Si$(CH_3)_2$-. PDMS is highly viscous fluid at room temperature but becomes flexible solid-like by cross linking after soft baking. In order to prepare a PDMS device, liquid is poured onto a master having the inverted structure on it (i.e. a trench in the master will produce a mesa on the PDMS device) as shown in Figure 4. The master can be prepared using different techniques such as photolithography on thick negative SU-8 photoresist, solid surface machining,[47], PCB technology[48,49] etc.

The arrangement when baked at ~80 °C for 2 hours successfully produces the crosslinking. After baking, the PDMS device can be peeled off from the master and used as a free standing, optically transparent device. The device with the feature can be bonded to another PDMS slab or glass surfaces that will provide rigidity to the device and maintain its optical properties. The bonding of PDMS surface to glass can be made irreversible by treating both the surfaces to plasma just prior to bonding. If the

surfaces are left in ambient atmosphere, they will lose the property of irreversible bonding.

The technology of soft lithography has produced a large variety of structures required for electrophoresis of different size particles[50], PCR chambers[15,20,21,51], microfluidic interconnects[52], microliter valves and pumps[53], membranes[47] etc. This technology has been extended to produce topologically complex 3-dimensional microfluidic systems[54] that have more than one plane of microfluidic channels. Multilayer PDMS structure has been demonstrated using bonding between two layers cast with asymmetric composition of silicone elastomer base and curing agent[30,53]. Two layers when prepared using base and curing agent in 5:1 and 20:1 ratios and cured through half the time can form irreversible bonding between them when baked completely. This can be repeated to obtain stacking of many layers to form a bulk device. For devices with small features, an intermediate step of silanization (eg. Tridecafluoro-(1,1,2,2-Tetrahydrooctyl)1-Trichlorosilane) of the master mould is necessary to obtain easy release of the high aspect ratio structures.

5.3. *Bonding*

Bonding has been used by many groups to prepare a hybrid structure from two different kinds of materials. Silicon having good thermal conductivity but poor optical transparency is always preferred as the substrate for thermal devices. It has been used for designing conformal devices using semiconductor technology. Devices need to be sealed from top to avoid loss of fluid due to thermal evaporation and to eliminate contamination from foreign materials. Most of the silicon devices are bonded with an optically transparent medium on top to facilitate fluorescence detection in normal reflection geometry. Glass seems to be the best choice for this purpose because of its excellent optical properties. The top glass layer can easily be drilled to form access holes for sample loading and unloading. The glass surface has almost similar atomic properties to the silicon-dioxide that is used as the coating layer for silicon based bio-medical devices. Glass can be bonded to silicon or silicon-dioxide surfaces at relatively low temperatures under an electric field[32] using the arrangement shown in Figure 5.

An optically flat cleaned glass piece (Corning Pyrex #7740) is placed on the top of the silicon-dioxide surface and heated to ~500 °C. Depending on the temperature and thickness of the glass, bonding voltage can vary from 200 to 1000 V. The bonding can be performed in normal atmosphere using a hot plate or under vacuum. The time required for bonding can take 5–15 min, that can be determined by monitoring the bonding current. To assist bonding, small pressure is applied to the glass and silicon sandwich using a pin point electrode on the top glass surface which is connected to the lower potential of the supply. The anodic bonding technology retains the underlying etched features in either top glass or the bottom silicon surface. Infrared aligner can be used for precise alignment if the bonded surfaces have features that need to be placed accurately with respect to each other.

Figure 5: Schematic of anodic bonding to permanently seal silicon-glass devices.

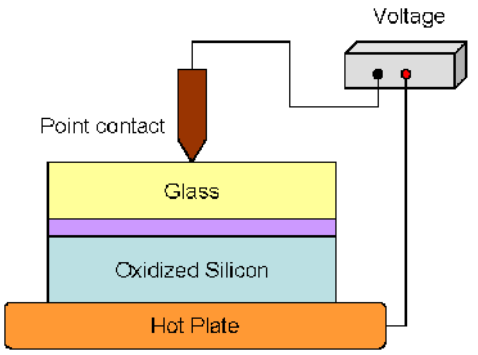

In case of soft lithography the sealing between two blocks or layers is achieved by reversible or irreversible bonding. A reversible bonding provided by simple van der Waals forces can withstand upto ~5 psi and can be watertight. This class of sealing is useful for microfluidics applications in low temperature and low pressure processes. Adhesive tapes can also seal devices with polymer surfaces such as PDMS reversibly. For irreversible bonding of PDMS devices two plasma treated surfaces are brought into contact as is described in the soft lithography section. In this technique it is believed that the plasma treatment generates silanol (Si-OH) groups on the top surface by oxidizing methyl groups of PDMS. Such a surface can form irreversible bond to another plasma treated surface of PDMS, glass, silicon, silicon-dioxide, polystyrene, polyethylene, or silicon nitride.

6. Various heating arrangements for miniaturized devices

As was described in the introduction, PCR mix contains components such as DNA template, short strand primers, dNTP, DNA polymerase, ions of Mg^{2+} etc. that need to be cycled through different temperatures for amplification. In order to cycle through temperatures, a suitable heating and cooling arrangement is required. The template DNA needs to be heated to ~95 °C in order to denature

completely in every cycle to ensure specific products. Higher temperature will ensure denaturation but will reduce the half life of the DNA polymerase and render it inactive beyond finite number of cycles. On the other hand, if denaturation temperature is too low, the reaction may yield either no product or non-specific products. Annealing temperature is defined by the sequence of the short ss-DNA and is another important temperature to be optimized in the chip. Higher temperatures will not allow annealing while lower temperature produces spurious products by non-specific annealing. Extension temperature is specific to the polymerase used in the solution, typical value being 72°C in most cases. Polymerase extension rate becomes slow on moving away from 72°C in either direction. Hence it is important to achieve correct temperature to make the extension process sufficiently fast in order to reduce the total stay time needed for complete extension of all the primer annealed templates. Commercial bench top machines, with slow heating and cooling ramp rate of ∼2°C/s for polypropylene tubes with ∼20–50 μL of sample, do not gain much by reducing the stay time. But in microchip PCR devices, ramp rates as high as 80 °C/s for heating and 40 °C/s for cooling have been achieved[55]. Total cycling time can be reduced drastically by using short stay times in these devices. Various types of heating mechanisms have been used by different groups to achieve faster heating and cooling rates, uniform temperature in the PCR chamber, optimized stay times etc. In general there are two kinds of heating mechanisms: contact and non-contact heaters.

6.1. *Contact heater*

In contact heater, the heater surface is directly attached to the microchip. This has the advantages of easy control and maximum heat transfer from the heater to the chip volume.

6.1.1. *Resistive heating*

Resistive heating has been the most commonly used heating arrangement in miniaturized thermal devices for a long time. Using existing semiconductor technologies, many groups have deposited metal films on silicon materials, that can dissipate sufficient power to produce ∼100 °C temperature on the chip surface. After the introduction of PCR chip by Northrup et al.[8] several groups have reproduced it using various intelligent chip designs. As a material for heater, they have used platinum[11,13,16–19,38,55,56], gold[9,10], aluminium[14], tungsten[30], indium tin oxide (ITO)[57] etc. Because of low adhesion of platinum and gold to the silicon surfaces, a thin layer (typically 10 nm) of promoter (Nickel/Chromium/Titanium) layer is first deposited. The metal heaters are deposited on the photolithographically patterned surface (usually meander shape) by thermal evaporation or sputtering followed by liftoff. Aluminium pads or conductive epoxy can be used to make connections to the external circuits. An important issue of using a metal film for heater is that it should form relaxed structures on the substrate and its properties (mechanical, electrical, thermal) should not change upon heating. Any kind of change in the metal film (thermal coefficient of resistance, thermal expansion etc.) will lead to irreproducible thermal profile in the micro devices. The position, size and shape of the heater have been optimized by many groups to speed up the reaction rate. For example, Liu et al. have used two independent heaters to achieve denaturation and annealing/extension temperature[30].

Several groups have analyzed the microchip thermal response using various mathematical models and softwares[12,17,18,56]. After pattern optimization, the micro heater can produce a uniform distribution of temperature in the microchamber[56]. Steady-state heat transfer equations are solved using FEA software such as Coventor Ware™ and ANSYS in order to simulate the temperature distribution inside the chamber. Zou et al. found the temperature of the mix to be within 0.5 °C of the heater and the reservoir to have maximum variation of 0.8 °C using steady-state heat transfer simulation[17].

Electrical isolation of the base silicon material from the heater is achieved by growing a thin layer of silicon-dioxide. This layer also helps in making the reservoir biocompatible for PCR. Ke et al. have integrated the platinum micro heater and temperature sensor into the micro chamber for efficient and rapid heating and cooling[18]. In order to protect the platinum surface from direct contact with the biological reagents, the surface is coated with a thin layer of silicon-nitride.

In order to achieve thermal isolation for the micro chambers, they are laterally isolated from the bulk material using air cavities. A thermally isolated silicon chamber produced considerable heating rate with an accuracy of ±1 °C using a fuzzy logic control program[18]. Suspending the reaction chamber on four beams to partially isolate it from the substrate, Daniel et al. could achieve a heating rate of 60–90 °C/s and cooling rate of 74 °C/s[11]. Yoon et al. studied the effect of groove size on the thermal response of the micro chamber[13]. Deeper grooves of same lateral dimension around the chamber inhibits more of the horizontal heat conduction. It concentrates more amount of heat efficiently to the chamber to increase the equilibrium temperature.

The transient response of the microchip improved drastically when the groove depth was nearly two-third of the thickness of the substrate. Power consumption was lowered by increasing groove depths. The cooling rate improved with groove depth indicating a possible convective path to release heat along the lateral direction through the bulk substrate.

A portable cycler was developed by Zhao et al.[56] using microcontroller based active proportional integral differential (PID) controller to regulate the temperature. A pulse width modulated (PWM) power source at 19.53 KHz supply the necessary power for heating. PWM based controller was also used by other groups[10] to acheive temperature accuracy of $\pm 0.5\,^{\circ}C$. In controllers using PID, individual parameters need to be optimized depending on the thermal load to obtain fast ramping without overshoot[9,14,16,17,40,58].

Doped polysilicon films have been integrated in the micro devices for heater pattern[36,40]. An undoped 4800 Å polysilicon was first deposited using low-pressure chemical vapour deposition (LPCVD) on top of an insulator layer in silicon devices. This layer was then doped with phosphorus to attain approximately 15.8 Ω sheet resistance. Using reactive ion etching (RIE) the layer was patterned into a parallel resistor grid and protected using a 5500 Å silicon oxide layer. Performance of the polysilicon heater was calibrated against a Type-K thermocouple and platinum resistance. Thermal coefficient of resistivity (TCR) of the heater was found to be $5.7 \times 10^{-3}/^{\circ}C$ and the resistance/temperature response was extremely linear in the PCR temperature range[36].

6.1.2. *Peltier block*

Some groups have used Peltier elements to control heat transfer to the silicon-glass microchip[34,39]. In this arrangement, the chip is heated or cooled depending on the direction of the current flowing through the peltier junction. This technique has been used by Anderson et al.[37] to perform chip-based detection of mutations in a 1.6 kb fragment of a HIV genome from a serum sample containing as small as 500 copies of the RNA. Lin et al.[58] used a Peltier block to cycle a silicon-glass device for amplifying complementary DNA (cDNA) molecules of C virus. Khandurina et al.[59] used dual thermoelectric Peltier elements to sandwich a 10–20 μL glass microchip. The bottom Peltier element was in contact with the chip surface covered by a drop of mineral oil while the top Peltier block was coupled only through radiation and was allowed to overshoot the temperatures. Chromel/alumel (Type-K) thermocouple embedded into the bottom Peltier block was used to measure and control the set points.

Erill et al. compared indirect Peltier heating with a polysilicon resistive heater embedded on the chip[36]. Apart from establishing differential temperatures using parallel junctions, Peltier blocks also produce radial gradients up to $2.5\,^{\circ}C$ for a 30×30 mm^2 area. If the devices are large, a copper plate is necessary for more uniform heating. In the above work, a 1 mm thick oxygen-free copper plate was used to produce $0.5\,^{\circ}C$ gradients. On comparing the PCR results between the direct (on-chip) heater and indirect (Peltier) heater, Erill et al found that direct heating outperforms the indirect one. While the indirectly heated chip consumed 12.3 W to produce $5\,^{\circ}C/s$ heating and cooling rates with the cold side of the Peltier at $55\,^{\circ}C$, the directly heated chip could produce $15\,^{\circ}C/s$ and $5\,^{\circ}C/s$ heating and cooling rates respectively using only 2.8 W power. On the other hand, the Peltier chip showed slightly improved amplification efficiency compared to the resistively heated chip. Probable reason might be the sluggish ramp rates and the strong overshoot present in the Peltier chip that increases effective stay time.

6.2. *Convective cell*

Steady circulatory flow of fluid between multiple temperature zones is another way of carrying out the thermally activated PCR process. Krishnan et al. demonstrated the use of Rayleigh-Bérnard convection cell to obtain thermal patterns that are suitable for PCR amplification[60]. The convective cell was made by drilling through plexiglass cubes with various aspect ratios and held between two water cooled plates maintained at desired temperatures. Flow patterns for different aspect ratios and Rayleigh numbers were studied from aqueous suspension of fluorescent latex microspheres. The flow moves the fluid packets through the different temperature zones that will enable the solution to go through the three steps of denaturation, annealing and extension. A 295 bp DNA segment was amplified in a cavity with height $\sim$1.5 cm and diameter $\sim$1.5 mm, and convection created by two plates at $97\,^{\circ}C$ and $61\,^{\circ}C$. Similar convection cycling was demonstrated in a slightly modified laminar geometry by Braun et al.[61]. A 20 μL cylindrical chamber was formed with two coverslips separated by a silicone spacer. The centre of the cell was heated using a focussed 1480 nm infrared laser (75 mW dissipated power) while maintaining the outer diameter at $52\,^{\circ}C$. The heating power was adjusted for optimum convective condition producing best amplification efficiency. High dissipation of IR power produced bubbles near the periphery of the chambers that prevents proper

annealing and extension of the templates. The cell was verified to produce exponential amplification over 5 orders of magnitude of initial template concentration. Amplification was imaged using SG fluorescence near the cell periphery.

6.3. *Solution heating*

As a possibility of direct heating of the PCR mix, Heap et al.[62] have used electrolyte resistance for heating. The technique is based on the fact that the PCR amplification buffer contains electrolytes that carry the charge while the viscosity of the liquid resists the current. The PCR solution becomes a 'wire' that is heated inside the glass capillary. The heating source was a 60-Hz 0–1000 V_{rms} power supply. The supply is connected to an acrylic reservoir using platinum wire electrodes. The reservoir is filled with 250 mL buffer. Amplification is carried out inside a capillary tube with flared ends, held between two reservoirs. Porous polyvinylidine fluoride frits form the bridge for electrical conductance and is held in place with a rubber sleeve. A dialysis tube is placed between the sample and the frits to prevent loss of the reagents out of the capillary tube by diffusion while allowing ion transfer with the buffer reservoirs. During thermal cycling, heating of the sample in the capillary and the buffer inside the frits occurs at independent rates. The capillary was cooled by blowing ambient air across it from an air compressor. The sample solution was degassed in vacuum for 10 min to minimize bubble formation during heating. Presence of a bubble causes local high-resistance zones, which in turn can cause localized boiling and breaks in the electrical path.

6.4. *Non-contact heating*

Contact heating methods as described above need a heater in contact with the microchip volume. Though the heat transfer is very efficient it adds to the thermal mass of the chip. This is disadvantageous during cooling when the excess heater mass also needs to be cooled down. Hence the total analysis time can be reduced further if the heater is thermally coupled to the sample volume only during heating but the chip remains isolated in the cooling step. This can be achieved with non-contact heating techniques. The idea of non-contact heating will reduce fabrication steps and therefore the cost of individual chips. The heater source can be a permanent component of the cycler and need not be discarded along with the chip after every use. For future LOC devices that require thermal treatment at multiple sites on the device, a single heater can be spatially scanned.

6.4.1. *Hot air*

Use of hot air for heating the PCR mix was first demonstrated by Wittwer et al. [27]. A 1 KW nichrome heater produces the hot air that is circulated around the sealed capillary tubes that contained the 100 μL mix. In order to increase the cooling efficiency a solenoid controlled door opened up to vent the hot air. The thermal profile was found similar to those obtained by water-bath reactions. The instrument was demonstrated with amplification of 56-bp fragment of E. coli DNA. Hot air based thermocyclers have been recently used in the amplification of DNA template in plastic/glass capillary [7,63]. Temperature was controlled precisely with a variation of 0.4 °C at 94 °C and a variation of 0.2 °C at 72 °C and 56 °C. The capillary tube was loaded on a circular carousel and inserted into the cylindrical temperature control chamber using air flow through a wind duct with a 300 W heater. A fan was rotated at low speed during heating while the same fan at higher speed was used during cooling along with reduced heater power. The major drawback of the hot air thermocycler is the issue of independently controlled devices in small systems. Further, this technique consumes more power and is not suitable for portable systems.

6.4.2. *Infrared lamp heating*

An alternative method of non-contact heating is to use infrared radiation from a tungsten halogen lamp. The spectrum of a standard tungsten lamp covers the wavelength range of 350 nm to 3 μm. Water has specific absorption bands at 2.66, 2.78 and 6.2–8.5 μm. Since the PCR mix is mostly water with strong absorption in the 1–4 μm band, a filtered IR source can selectively heat the sample contained in microchambers. The technique has been demonstrated in borosilicate glass[35] and glass capillary[28]. A TTL modulated General Electric CXR tungsten lamp (with internal lamp temperature of ~3500 K reached in milliseconds) powered by a 5 V AC transformer was used to produce the heat by Oda et al.[35]. A proportional controller with the sensor temperature read by a copper/constantan thermocouple (with output of 1 mV/ °C) was used to maintain the temperature. It was found that a thermocouple with outer diameter of 0.005 inch, in contact with the PCR sample inside the glass tube inhibited the reaction. Hence the design was modified to a double microchamber configuration. In this design, one of the microchambers will contain the PCR sample for cycling without being probed by the sensor while the other dummy microchamber will have the thermocouple for temperature measurement. Position and thermal properties of both the

chambers are calibrated apriori. For thermal control, pulse width modulation was used. A ramp rate of 10 °C/s and 20 °C/s for heating and cooling (using compressed air) was achieved for 5 μL of PCR mixture in glass microchambers. The temperature was stable within ±0.3 °C at 94 °C and 72 °C and ±0.4 °C at 54 °C.

The same technique has been employed in nanoliter volume PCR inside a 8 cm long, 150 μm-i.d. and 375 μm-o.d. capillary by Huhmer et al.[28]. In this case the temperature was measured with a copper/constantan thermocouple (with 0.001 inch outer diameter) inserted inside another dummy capillary and placed close by. A part of the polyimide coating was removed from both the capillaries to enhace IR coupling. A long-wave pass filter with a 680 nm transmission cut off was placed between the capillary and the IR lamp to optimize wavelength selection and prevent photolysis of PCR components. The optimum focussing of the IR light to the microchamber using a lens arrangement produced 65 °C/s heating rate. The capillary material having major absorption bands at 3 and 4.5 μm can also contribute to the solution heating. The technique has been extended to polymeric material such as polyimide microchip by Giordano et al.[29]. Polyimide can be used for PCR devices since its glass transition temperature is ∼350 °C. The material is transparent in the 600–3000 nm range which makes it a good choice for radiative heating because the solution can be heated independent of the substrate. Heating rate of 10 °C/s using full lamp power and cooling rate of 10 °C/s without forced air was achieved. Polyimide chips showed successful amplification with the use of 0.75% polyethylene glycol (PEG) in the reaction mixture.

6.4.3. *Laser heating*

Radiative heating requires proper focussing of the source to a small area using IR compatible optics. The power coupling was stated to be strongly dependent on the relative position of the chip. The dummy chip with the sensor needs to be placed reproducibly in the same environment relative to the source and the reaction chip to maintain the same calibration. Focussing optics has been eliminated using laser heating by some of the groups[64,65]. Tanaka et al. used a glass microchip with 'Y' junction placed on a Peltier block. A diode laser of 10 mW power and operating at 635 nm wavelength was incident on top of the junction to locally heat the sample inside the microchannel. More effective heating can be achieved by directly heating up water molecules using 1064 nm infrared radiation from a Nd-YAG laser, without any effect on the solute. A focussed beam with 500 μm diameter heated 10 nL of solution in the microchannel. Temperature was studied as a function of laser power, irradiation time, and intensity. The temperature measurements were performed using a thermal lens microscope.

Slyadnev et al. used a reduced laser spot size of 150 μm from a 150 mW laser at 1472 nm wavelength to heat up solutions inside microchannels[65]. Temperature dynamics and spatial distribution inside the microchannel were studied using fluorescence-quenching technique of rhodamine 3B dye. At low flow rate the volume of liquid heated was similar to the irradiation volume but the hot temperature zone started to spread out with higher flow speed. Temperature dynamics study with different laser powers showed a heating rate of 67 °C/s and cooling rate of 53 °C/s using a Peltier block maintained at low temperature.

6.4.4. *Induction heating*

A microchip thermocycler was developed from our group by Pal et al. using magnetic induction field that can heat up MEMS devices to carry out thermal reactions[66]. The principle is based on the mutual induction between a primary coil and a magnetic ring or sheet. More details of this device and its performance are discussed in Section 9.

7. Temperature sensing

The success of integrated PCR systems depends on repeatibility of the temperature cycle. PCR being a thermally mediated process, it becomes important to heat and cool the system reproducibly to required temperature values. In doing so it is necessary to measure the temperature accurately and provide appropriate feedback to the controller unit. It has always been a challenging task to measure the temperature inside the small volume of micro-devices without perturbing the system. Temperature read-out is an essential component in micro-chip technologies since this can affect many other important parameters such as the pH of the buffer solution, enzyme life time, annealing efficiencies, bubble formation etc.

Many of the early works have been carried out using bulk thermal sensors such as thermocouple[10,27,28,35,65,66] and platinum-100 resistor[57] fixed to the side of the reactor used for PCR. Other methods are discussed below.

7.1. *Metal film sensor*

Attempts have been made to use underlying metal films in planar configuration along with the heater layer for sensing temperature. Metals having good thermal coefficient of resistivity such as platinum[11,13,16–19,38,55,56] and gold[9] have been

used as sensors. If the chip heating element and the sensor are of the same material, fabrication can be simplified by simultaneously doing lift-off for both the layers. Many research goups have used different shapes such as meander[11,16] and circular[9] patterns. Since the sensing layer material is in contact with the chip, it is expected to be less affected by external environmental fluctuations and at the same time sense the reservoir temperature more accurately. This sensor, being in permanent contact, is also more reliable and reproducible. In most of the micro devices, sensor and heater are designed on the back side while the sample to be cycled is loaded in the micromachined reservoir on the front side of the device. The sensor readout is therefore not directly equal to the reservoir temperature. Attempts have been to minimize this difference by reducing the amount of material between the sensor and the reservoir bottom. Sensor materials have been shown to inhibit PCR reactions when used in direct contact inside the chamber for measuring in-situ temperature. Most of the recent designs optimize the sensor position using simulation results[18]. One major drawback of this technique is cost. For example, platinum, being very expensive, is inappropriate for single usage disposable devices. Erill et al. have used polysilicon sensing for micro PCR devices[36,40]. There is a need for cheaper sensor materials such as thermistor paste, simpler fabrication techniques, better material compatibility and improved thermal response.

7.2. *TLC sensor*

Thermochromic liquid crystals (TLC) are mainly derived from cholestrol and are capable of displaying a range of visible colours. Typical response is red at low temperature and spans through orange, yellow, green, blue and violet as the crystal is heated. Crystals are translucent beyond the temperature bandwidth. In order for TLC to serve the purpose of temperature sensor in microfluidics and micro reactors, they have been encapsulated in polymer to make them resistant to fluid, moisture, dusts, and less sensitive to viewing angle. A CCD with linear response in the range of TLC emission wavelength can be used to image the change. CCD with individual RGB pixels can give better sensitivity and clearer picture of the fluid[67]. Noh et al. calibrated liquid crystal (LC) filled silicon microchambers sealed with mineral oil and polymer epoxy to prevent evaporation[68]. Chaudhari et al. measured thermal uniformity and time constant using different sets of TLC near 55 °C and 95 °C[69]. The disadvantage with TLC is that low temperature sensitive TLC has higher density compared to the high temperature one. This can cause the crystals to measure the reservoir bottom at low temperature and top at high temperature. The temperature sensitivity ranges are very narrow and hence it is not possible to cover the wide range of temperature that is required in a PCR cycling using a single TLC.

7.3. *Fluorometric sensor*

In this technique, fluorophore molecules are added to the fluid and the fluorescence intensity is recorded using fluorescence microscope or CCD camera. Spatial resolution is determined by the microscope optics and the temporal resolution is maintained by fast data acquisition from the detector. High signal to noise ratio of the fluorescent dye allows its use in dilute amount without affecting the sample chemistry. Since fluorescence intensity is temperature dependent for most of the dyes, they can be used as sensors. The fluorescence optics can be designed to accomodate more than one dye to be investigated. Ross et al.[70] have demonstrated the use of Rhodamine B to measure liquid temperature ranging from room temperature to 90 °C with precision of 0.03 °C near room temperature and 0.07 °C at elevated temperature of ∼85 °C. The system was capable of measuring microfluidic temperatures with 1 μm spatial resolution and 33 ms temporal resolution. The dye has been used to record the transients inside microchannels with different sizes and shapes of the channels.

Recently Mondal et.al.[71] demonstrated a novel way to use SYBR Green fluorescent dye for both temperature control and monitor DNA amplification in a microchip PCR system. This method simplifies the optical design of the fluorescence detection unit. Fluorescence feedback PCR was shown to produce the correct product with the same efficiency as that with temperature feedback.

7.4. *Other methods of temperature sensing*

Non-contact Raman spectroscopy utilizing the Raman spectrum of O-H vibration mode of water has been used to measure in-situ temperature of fluid inside microchannels [72,73]. The temperature inside the channel was found to be lower by 0.2 to 1.4 °C compared to the chip.

Nuclear magnetic resonance (NMR) is another non-contact technique used for temperature sensing. NMR spectroscopy is well known for its ability to characterize molecular structure. Only after the development of reduced diameter radio frequency (rf) transceiver coils, there have been improvements in the mass sensitivity of NMR probes. These small scale pick up coils have enabled high resolution NMR detection in miniaturized devices. NMR temperature sensing has been implemented in

Figure 6: Continuous fluorescence signal of PCR cycles. The red curve corresponds to the single point detection of the PCR fluorescence as monitored at annealing temperature.

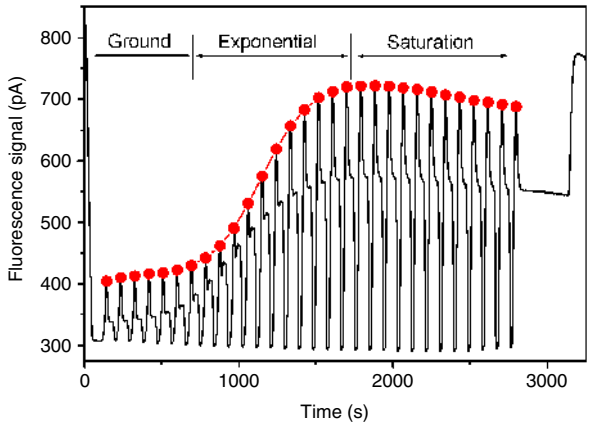

capillary by monitoring the proton resonance frequency of the which shows a strong linear dependence on temperature [74].

Heap et al. used solution resistivity to sense temperature during PCR amplification[62]. Since liquid viscosity decreases with increasing temperature, ionic resistance of the solution is directly correlated to its temperature. This allows direct monitoring of the fluid temperature, without any external thermocouples or devices.

Temperature can also be measured from the change in fluorescence life time when heated. Jeon et al.[75] used rhodamine-G labeled DNA oligomer to study the change in fluorescence intensity at different temperatures as a function of time. Two-photon excitation by a femto-second Ti:Sapphire laser was used to excite the fluorophore. The change in the fluorescence lifetime with temperature was found to be 42 ps/°C. Control experiments with free dye in solution was found to have no such dependence, confirming that the effect was from DNA attached to the fluorophore dye.

8. Use of SG fluorescence in miniaturized PCR devices

In conventional PCR protocols, DNA is first amplified in the thermocycler for 1–2 hours and then detected by electrophoresis in a gel matrix, which requires another 1–2 hours depending on the fragment sizes. In order to reduce this time, it is necessary to integrate detection technology along with PCR. One way to do this is by using fluorescence based detection that has been implemented in some commercial thermocyclers. Fluorescence based PCR detection uses either sequence specific probes (Taqman, FRET, iFRET, Scorpions, molecular beacons) or sequence independent intercalating probes (Ethidium bromide, SYBR green I and Picogreen). In sequence specific probes, fluorophores are designed along with bases that are complementary to a small part of the template. In case of sequence independent probes, the dye molecules intercalate or bind to the major grooves of the ds-DNA depending on the dye to base pair ratio[76]. Among intercalating dyes, the most commonly used in real time PCR is SYBR green I (SG) dye. The dye gives green fluorescence when excited with blue light and this is monitored once in every cycle to verify the amplification. The fluorescence shows a rising envelope with cycle number when amplification is successful, the exact shape depending on inter cycle amplification kinetics. Fluorescence is higher when dye molecules are intercalated in ds-DNA than when they are free in solution. Thus fluorescence intensity is a measure of ds-DNA concentration.

8.1. *Fluorescence monitoring of PCR*

Real time PCR using fluorescent dye was demonstrated in the year 1992 by Higuchi et al.[77] using ethidium bromide in the PCR mix. The tubes were imaged through red filter using a UV excitation source. The amplification was continuously monitored using fibre optics to excite and collect the fluorescence from the ongoing PCR to a spectrofluorometer. The profile shows the fluorescence following temperature cycling (see Figure 6): fluorescence increases at annealing temperature (55 °C) and reduces at denaturation temperature (95 °C). At 95 °C all the ds-DNA are denatured to form ss-DNA, releasing the dye molecules to be free in the solution. This produces a constant background at denaturation temperature independent of the cycle number and ds-DNA concentration. At annealing temperature the fluorescence is higher as the primer is annealed to the ss-DNA template. Since the number of template molecules increases with cycle number the annealing fluorescence intensity is also expected to increase. In conventional real time PCR, fluorescence values are recorded at a fixed temperature in every cycle. The values when plotted as a function of cycle number are shown in Figure 6 (red curve). A CCD based detection was used by Higuchi et al. to record the fluorescence from tubes in the annealing or extension phase and analyzed by image processing software to study the influence of different concentration of polymerase, primer, KCl and PCR inhibitory hermatin[78].

Theoretically the amplification is expected to follow a 2^n law, but experimentally an efficiency $E(\leq 1)$ can be defined such that $N = N_0(1+E)^n$,

Lock-In amplifier: An instrument which amplifies only the component of the signal at the same frequency as a particular reference signal. This technique excludes noise at all other frequencies and can be used to detect very small signals in the presence of large background noise.

where N_0 and N are initial and final amount of ds-DNA after the nth cycle. This law holds only in the exponential phase of the amplification but not in the late saturated phase. In the early ground phase the change in the fluorescence signal is much lower than the detection sensitivity while in the late saturation phase the amount does not increase further due to chemical limitation. Beyond certain number of cycles, all the important chemical ingredients such as dNTP, primers, polymerase etc. are exhausted and there is no further amplification. Many theoretical models have been developed to explain the nature of the fluorescence envelope. Liu et al. have demonstrated a better fit to the amplification envelope using a dynamically changing efficiency parameter[79]. The amplification efficiency have been measured to vary between ~40% and 90% depending on the PCR mixture optimization. Arezi et al. have studied the amplification efficiency of thermostable DNA polymerases as a function of SG concentration, length of the product and percentage GC content[80]. They reported a lowering in the amplification efficiencies for longer lengths and higher percentage of GC content for most of the polymerases. Real time fluorometric cycler for PCR has been established for glass capillaries using various kinds of dye molecules[63,81–83]. Quantitative PCR has been performed on microfabricated devices as well[84–86]. A detection block inspired by the DVD (digital versatile disk) head has been developed to fit portable devices with sensitivity in the low nanomolar range[87]. The fact that the microchambers are often made from silicon substrate was exploited by Webster et al. to fabricate the photodiode in the substrate silicon itself that measures the fluorescence emitted from eluting molecules[88]. A thin film interference filter coating was used to allow only a specific emission wavelength to strike the detector. SG labeled ds-DNA was analyzed by electrophoresis in the microchannel fabricated on this device. Small scale integration of the detection unit enabled the development of hand held real time thermal cycler for pathogen detection[89].

As has been discussed above, denaturation and annealing are instantaneous processes once the correct temperature is reached while the extension is not. The extension stay time depends on the polymerase activity rate, template size, chemical concentration, temperature etc. Hence in microchip PCR protocol with faster ramp rates, optimization of the stay time can reduce the total time. This optimization is not possible in single point data acquisition system which acquires fluorescence intensity once every cycle. As has been pointed out in many real time continuous data reports, the extension phase of the PCR cycles show a gradual rise in fluorescence with time[81,90,91]. In order to perform the optimization, it is necessary to acquire intra-cycle fluorescence data at sufficiently fast rates. From our group, we have demonstrated a fast data acquisition system based on lock-in technique for SG fluorescence dye[92] which is described in Section 9.

8.2. *Fluorescence from microchip*

SG has been used to record continuous fluorescence data from microchip PCR[9,93,94]. In case of devices with high ramp rates, the liquid can have a non-equilibrium temperature distribution leading to convection currents inside the reservoir. Hence it is important that the entire chip equilibrates before the temperature is switched to the next set point. Since extension is the rate limiting step when fast protocols are used in microchips with high ramp rates, the extension rate should be optimized to reduce the total stay time. The variation in the extension rate was measured in an inductively heated silicon-glass microchip with 3 μL volume by Mondal et al. to show the effect of temperature on extension step[94]. A temperature of 75 °C was found to maximize polymerase activity rate in the microchip for two different sizes of template. A dynamic optimization protocol was compared with respect to the fixed time cycling using 15, 30, 60 and 120 s for extension steps. In case of variable stay time experiment the fluorescence envelope reaches the maximum faster when compared to the fixed stay time protocols. The power of the technique is the ability to monitor individual extension steps throughout the PCR cycles. This technique can eliminate the run-to-run variation in microchip PCR by using intra-cycle feedback.

8.3. *Melting curve analysis*

Use of SG in the PCR mixture allows product confirmation after the completion of amplification by using product melting analysis. Every ds-DNA has a melting temperature T_M beyond which the double helix is not stable and all the hydrogen bonds break down to form two complementary ss-DNA. Since SG molecules intercalate to ds-DNA only, melting is expected to show a sudden drop in fluorescence as the temperature is ramped through the melting temperature T_M. In order to obtain the correct T_M value, the temperature is ramped very slowly (~0.1 °C/s) upto 95 °C and the fluorescence is continuously monitored. The fluorescence first shows a gradual drop due to the intrinsic temperature coefficient of the dye but decreases suddenly at T_M and further becomes constant due to absence of any bound SG molecules

Figure 7: Melting curve analysis of PCR product. The fluorescence (red) and its derivative (black) are plotted to highlight the melting transition.

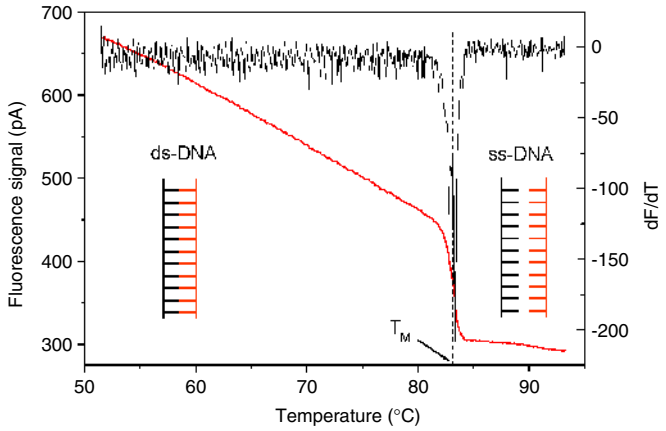

Figure 8: Schematic (left) and photograph (right) of a silicon-glass PCR device.

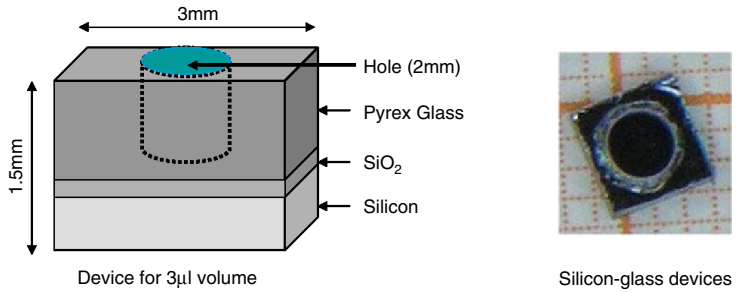

Melting of DNA: ds-DNA exists in helical form by forming hydrogen bonds between its two complementary strands. At elevated temperature, the hydrogen bonds become unstable and the DNA exists in the form of two ss-DNA. This state of the DNA is said to be denatured and the process is called denaturation or melting. In practice the temperature is ramped slowly at 0.1 °C/s to obtain the melting point T_M of the DNA.

(as shown in Figure 7). Derivative of this curve around T_M will show a peak with certain width. The T_M depends on many parameters such as template size, percentage of GC content, SG concentration, salt concentration in the solution, temparature ramp rate etc[95]. Provided the ramp rates are slow, observation of the correct T_M will confirm the amplified product[81].

Even when using SG in multiplex PCR that produces more than one kind of DNA, melting curve analysis can be used to identify individual products[96,97]. For two different sizes of ds-DNA and different GC content, the melting curve can be fitted with two peaks in the derivative plot provided they are well separated. In case of multiplex DNA melting, the SG concentration has to be carefully adjusted to obtain both melting peaks, as was shown by Giglio et al. using multiplex assays for *Vibrio cholerae* and *Legionella pneumophila*[96]. This study showed a preferential binding of SG during melting and failure to detect multiple fragments with limited amount of SG molecules. This work suggests that optimization is required for multiplex PCR to avoid false results in diagnostic studies. Increasing SG alone will hamper the reaction efficiency unless Mg^{2+} is also optimized[98].

Since the melting point is fairly sharp and unique for a given DNA, it can be used as a "temperature marker" in microchip devices. Assuming homogeneous temperature inside the microchip, melting of a known DNA can be used to calibrate as well as characterize a micro device[9,16,94]. The spread in the derivative peak can be related to the thermal uniformity of the device. Mondal et al. used three different ds-DNA with melting points ranging from ~78 °C to 91 °C to calibrate the reservoir temperatures[94].

9. Examples of microchip PCR devices

In this section, we present details of fabrication and characterization studies of Silicon-Glass and PDMS devices fabricated in our laboratory. The former used induction heating while the latter used simple resistive heating. We also discuss the design, fabrication and testing of a fluorescence detection unit that was used to detect real time fluorescence from both polypropylene tubes in commercial thermocyclers and the microchip devices.

9.1. *Silicon-glass device*

The device consisted of a 1 cm square glass (Corning Pyrex #7740) piece that had a 2 mm drilled hole. After the drilling, it was etched to 1 mm thickness to remove the stress around the hole. The glass was anodically bonded to an optically polished 500 μm oxidized silicon piece. The oxidized surface of the silicon mitigates adverse surface related problems. The device was finally diced to 3 mm $\times$3 mm size. The hole at the centre forms a reservoir for ~3 μL sample volume. Figure 8 shows one of the silicon-glass devices that was used for microchip amplification reactions described below.

The optimized induction heating circuit[94] shown in Figure 9 uses a 0.2 mm thick copper sheet of diameter 10 mm as the secondary (900 nH) placed on an air cored primary coil. The primary inductor forms an LC tank circuit with a 4.7 μF capacitor in parallel, that is driven by a single HEXFET power MOSFET (IRFP150N) and powered from 10 V high current supply. A thermocouple is soldered at the back of the secondary and read using an AD595 amplifier. The voltage is compared with computer specified set points and digitally 'AND'ed to a 75 KHz square pulse. The output is fed to a driver (IR2110) that switches the MOSFET. The 3 μL silicon-glass chip was fixed to the secondary

Figure 9: Schematic of induction heating circuit. Components used are: thermocouple amplifier (A), comparator (B), digital AND (C), timer (D), driver (E), power MOSFET (F) and LC tank circuit with primary coil and capacitor.

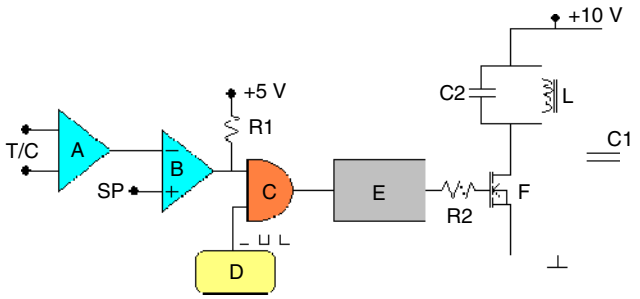

Operational amplifier: Operational amplifier (OPAMP) is a high gain voltage amplifier IC, used typically with negative feedback. It can be used as a differential amplifier where difference of the inputs is amplified to give a single ended output.

using heat sink compound. The chip was filled with 3 μL PCR sample. Simple on-off control produces thermal stability within ± 0.1 °C and heating and cooling rates of 25 °C/s and 2.5 °C/s respectively. The temperature profile during typical PCR cycling is shown in the inset of Figure 13 for the first few cycles. The microchip reactions were carried out with short stay times at denaturation and annealing but the extension stay time depends on the template and the temperature used. The chip thermocycler was integrated with a real-time fluorescence block to optimize the reaction conditions.

PCR sample is almost water and needs to be heated to ~95 °C for complete denaturation of ds-DNA. At this temperature a small volume of liquid can vapourize instantly and hence needs to be sealed properly. We have tried using epoxy PCR compatible tape for thermal sealing. These tapes need to be held in position with sufficient amount of pressure to ensure sealing. This arrangement blocks the optical path and is not suitable for fluorescence detection. The tape was therefore replaced by an optically transparent mineral oil with high boiling point (Mineral oil, Sigma). About 4 μL of this oil was spread on the top of the device after filling the reservoir with the PCR sample. This allowed detection of fluorescence and complete recovery of the amplified sample after nearly 30 cycles.

Figure 10: Schematic of the fluorescence block used for SYBR green I dye.

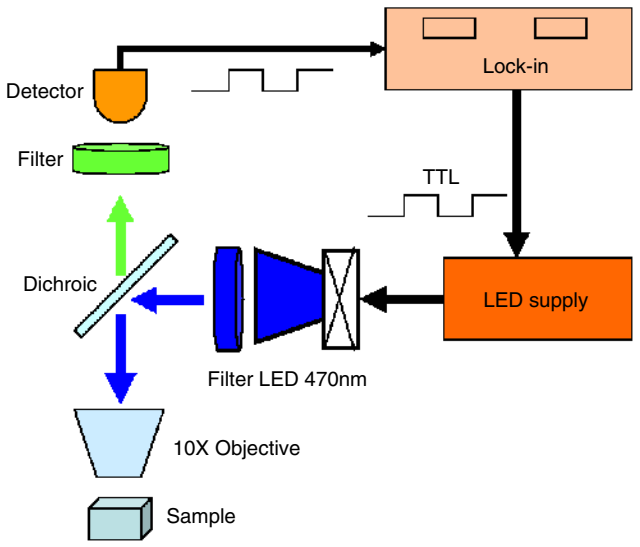

9.2. *PDMS devices*

Small devices were fabricated out of PDMS elastomer using moulds as described in the soft lithography section. We created small inverted reservoir structures resembling standard polypropylene PCR tubes in the master mould which were then transferred to the PDMS layer. The PDMS devices were then diced into smaller sizes to reduce excess mass around the well. The devices were bonded onto a glass slide with aluminium heater pattern on it. The metal pattern was covered by a thin spin coated layer of PDMS that prevents the metal surface coming into direct contact with the DNA solution. The reservoir was filled with 3 μL of DNA solution with SG for checking melting curves. The solution was overlaid with 10 μL of mineral oil and a Type-K thermocouple was inserted into the reservoir to sense the solution temperature. The thermocouple was connected to the amplifier AD595 and its output was compared with computer controlled set points using a comparator LM311. The temperature was stabilized using simple on-off control.

9.3. *Fluorescence instrumentation*

A fluorescence block consists of an excitation source, a collection arrangement and detection unit specific to the dye molecule. SG molecule has excitation and emission peaks at 470 nm and 520 nm respectively. A fluorescence block was built using a high power blue light emitting diode (LED) excitation source that was filtered through a blue band pass filter (450–490 nm) having ~80% transmission (Figure 10). The emission path was built using a high pass filter (515 nm) with $\geq$90% transmission to allow light with wavelength greater than 515 nm. The filtered light was then collected using a silicon photodiode. The two optical paths were coupled in the perpendicular direction using a dichroic mirror, that has higher transmission for longer wavelengths. The dichroic is placed at 45 ° to the excitation such that it reflects all the blue light into the PCR mix using a focussing arrangement. At the same time,

Figure 11: Real time PCR curve of different dilution of TGFβ1 cDNA in polypropylene tube after subtracting the background. The top figure shows the fluorescence envelope for 40 cycles for different amount of initial template concentrations as explained in the figure legend. Bottom figure shows the threshold cycle number plot as a function of log of initial template number.

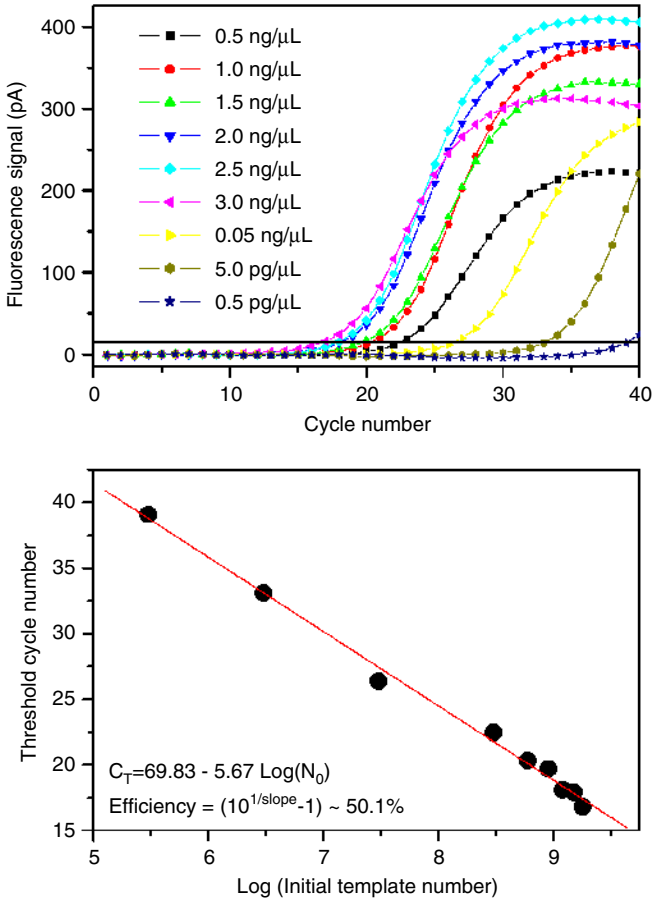

the emitted green light is allowed to pass through the dichroic to be filtered and detected. The focussing and collection was done by using a 10× objective.

In order to use lock-in detection, the blue LED supply was triggered using a reference TTL (190 Hz) from the lock-in amplifier (SRS830). Assuming negligible time delay in the fluorescence, the emission from the SG at 520 nm should also be at the same phase. The photocurrent when fed to the lock-in amplifier and locked to the TTL frequency can be detected at very low signal levels.

The efficiency of the PCR is determined by its ability to produce the specific product in high yield with minimum number of cycles. The amplification efficiency can be influenced by a number of factors such as target and primer lengths, their sequence, buffer condition, cycling conditions, DNA polymerase etc. Improvement of the efficiency by a small factor can lead to considerable increase in the yield. Earlier, researchers have used end point analysis to determine efficiency of the polymerase by adjusting cycling conditions. However end point analysis can sometimes be misleading as the reaction yield saturates after a certain number of cycles. Amplification can be best studied in real time PCR systems where fluorescence data is monitored during the cycling. Experimentally the amplification efficiency (E) is less than one and this leads to the amount of product after nth cycle as $N = N_0(1+E)^n$ ($E = 1$ is the ideal situation where the amount doubles every cycle). When the fluorescence number increases beyond a noise level after a threshold cycle (C_T), the number becomes $N = N_0(1+E)^{C_T}$. Thus a plot of C_T versus the log of initial target copy number is a straight line, with a slope m equal to $-[1/\log(1+E)]$ corresponding to amplification efficiency of $E = 10^{[-1/m]} - 1$.

In order to test the sensitivity of the home-made fluorescence block, TGFβ1 cDNA cloned in the plasmid BlueScript was used as a template. This DNA was used in different dilution and 3 μL volume was loaded in a polypropylene tube with 6 μL mineral oil for sealing. The tube was cycled in a commercial thermocycler for 40 cycles and fluorescence was recorded continuously every 1 s. In order to obtain the curve in Figure 11 we pick the fluorescence number at the annealing temperature and correct for the background drift using the base value of first few cycles. The threshold cycle number was calculated using a reference fluorescence number of 15 pA which is much higher compared to the background. Threshold cycle number when plotted against the log of initial template number shows a straight line for the dilution values used in this experiment. The efficiency was calculated to be 50% in this case.

Another important check is to compare fluorescence data with gel electrophoresis. Control experiments were designed with no DNA template and using a DNA template non-specific to the primer. In both these cases fluorescence remained unchanged for 40 cycles. The positive sample, on the other hand, clearly shows an amplification under the same reaction conditions. The products were checked by melting curve analysis and in agarose gel. Figure 12 shows the fluorescence signal and gel photograph of these control experiments that were carried out in standard polypropylene tubes.

Extension experiments were performed at different temperatures and the polymerase activity was found to be strongly dependent on temperature. Using continuous intra-cycle fluorescence measurements, polymerase activity was estimated *in-situ* during the PCR reaction and found to be well within the specified value from the vendor[92].

Figure 12: Fluorescence compared with gel electrophoresis. Lane no 1 is negative mix (without DNA). Lane no 2 is mix with non-specific DNA. Lane no 3 is positive sample. Each mix underwent 40 cycles of amplification. The inset shows the agarose gel photo for the three samples.

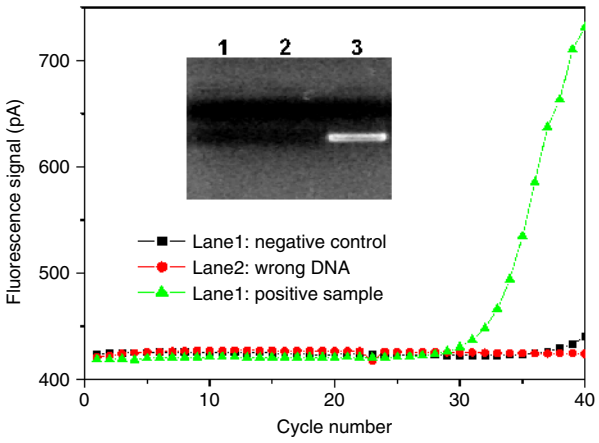

9.4. *Fluorescence based testing of the microchip devices*

Figure 13 shows an example of successful PCR amplification in the inductively heated silicon-glass chip as monitored by fluorescence. Figure 14 shows the melting profile of two different kinds of DNA when melted in a PDMS device with tube-shaped reservoir. The set point of the control circuit was increased from 0.50 V to 0.95 V with a ramp rate of 0.001 V/s and the fluorescence was recorded every second. The device was heated using an aluminium pattern of ∼18 Ω resistance with a 12 V supply. The device was later modified with a planar geometry to improve thermal uniformity. This design shown in Figure 15 was heated using a ∼8 Ω aluminum pattern. In the present chip design, no external thermal sensor could be used to sense the in-situ liquid temperature. For melting curve analysis, the set point was ramped from 1.0 V to 2.5 V with a rate of 0.005 V/s (shown in Figure 15). The fluorescence signal has reduced in this design due to the very shallow reservoir.

Figure 13: Real time fluorescence signal from silicon-glass device. The fluorescence showing successful PCR amplification of pUC18 DNA in microchip using induction heating. The inset shows the temperature profile as measured by the thermocouple attached to the secondary.

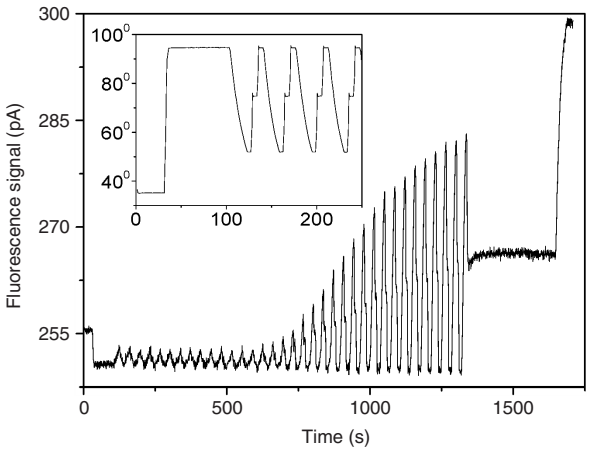

10. Integrated DNA analysis systems

Among the established clinical practices for pathogen detection, culture and extraction of biomaterial from blood samples is an important step in the protocol. Various chemical methods exist to perform the extraction of DNA from blood that contains many components that inhibit PCR. Millar et al. have compared various methods for DNA extraction from blood and verified them using PCR[99]. An important issue when using culture procedure for PCR is that the sample should be completely free from contaminant DNA and PCR inhibiting chemicals used for DNA extraction. Chemical extraction procedures are performed on large volumes which are unsuitable for miniaturization, hence new techniques have been developed by various groups based on silicon technology.

Most of the microchip PCR protocols require DNA purification prior to amplification to remove possible PCR inhibitors. Some groups are working towards the use of on-chip DNA purification to be integrated with other processes. The common protocol for DNA purification is based on adsorption of DNA on solid silica particles by surface forces and then elute them in solution. Breadmore et al. used this technique in small scale to purify DNA using silica and silica-sol gel hybrid particles in microchannels[100]. It was reported to have 67% recovery of λ-phage DNA and 68% chip-to-chip reproducibility evaluated over minimum of three different extractions. The extraction process was made fast by increasing the flow rate of the buffers (maximum of 250 μL/hour) through the chip at lower pH. At lower pH (best at pH 6.1) there is a reduction in the extent of protonation of the silanol groups on the bead surfaces, thus increasing electrostatic repulsion between DNA and silica surface but providing more number of such surfaces for increasing binding sites. DNA extraction from direct blood sample using sol gel electrophoresis took 15 min and was checked for successful amplification using PCR.

Wilding et al. demonstrated isolation of white blood cells from whole blood sample using different

Figure 14: Melting curves of DNA in PDMS device with tube shaped reservoir.

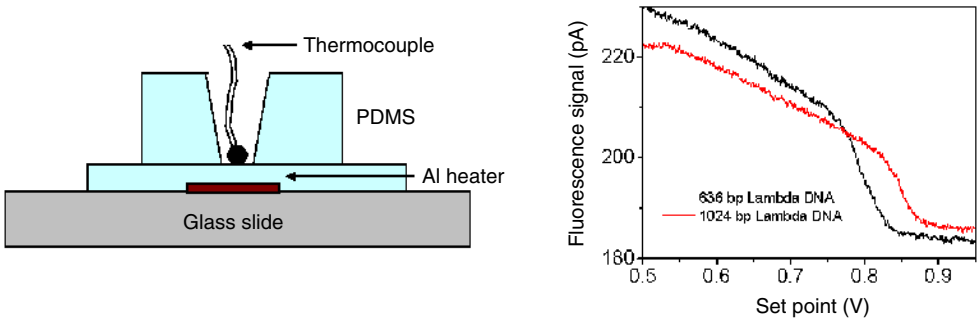

Figure 15: Melting of DNA in modified PDMS device with planar reservoir.

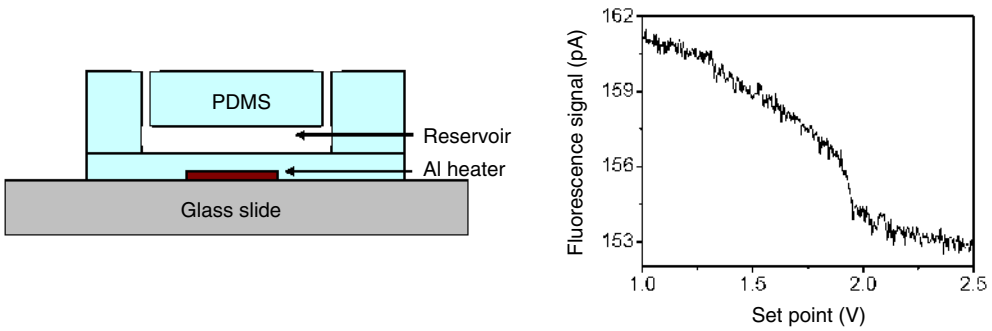

kinds of silicon microstructures[101]. The group tested different forms of post and weir-type structures inside the microchannel interacting with velocity fields. These structures allowed all material except white blood cells to pass through the traps. Hemoglobin in red blood cells is an inhibitor for PCR and after its removal, PCR shows successful amplification. PCR is performed on the same chip after releasing DNA from the trapped cells during initial high temperature step. Similar silica based structures have been used by other groups to isolate and extract DNA from cells for carrying out amplification[93,102,103]. Automated systems performing amplification, separation and detection in capillaries using blood have been demonstrated by Zhang et al.[104]. The blood sample was treated with formamide and incubated at 95 °C for 5 min and loaded in eight-array multiplex PCR system using air thermocycler. Programmable syringe pumps maintained the flow while control and distribution were achieved using multiplexed liquid nitrogen freeze/thaw switching valves. Electropherograms after PCR were compared with standards using multiple capillaries. The use of "electrophoretic valve" by Woolley et al. simplified the design that is easier to integrate on the chip[10]. A viscous hydroxyethylcellulose (HEC) sieving matrix at the interface of the PCR chamber and the electrophoretic channel prevented the movement of the PCR components to the channel during thermal cycles. Use of high voltage after the completion of amplification allowed DNA to enter the channel for electrophoresis.

Attempts have also been made towards sequencing of PCR products in small volume samples that can fit the requirement of miniaturized PCR devices. Hashimoto et al. used serially connected glass capillaries to perform amplification, introduction of reagents, cycle-sequencing reactions, purification of the sequencing ladder, injection and size separation[105]. They used microsyringe pump technology for fluid flow in the capillaries. The performance of the complete one step sequencing of 257 bp region in human Y chromosome DNA was demonstrated in ~1.6 μL volume that took ~4 hours time. In an attempt to enhance the speed of these devices, more efficient components are being developed for cell lysing, fluid transport, flow control, micro mixing, thermal management, electrophoretic separation and detection. For

example, lack of transverse component in laminar flow shows poor mixing of the components while use of AC voltage has been used to show better mixing[106]. This increased efficiency of the device for cell lysis and mixing is shown to produce higher signal. Steps such as cell sorting, cell lysing and purifying might require use of nanoparticles, magnetic field etc to increase process efficiencies. Very little progress has been made in testing and incorporating all these steps together on a single platform. Liu et al. developed a fully integrated microchip incorporating microfluidic mixers, valves, pumps, channels, chambers, heaters, and DNA microarray sensors[107]. The device consists of all on-chip components to have minimum human intervention that can analyze raw biofluids directly as it is capable of performing cell capture, preconcentration, purification and lysis. The mixing was achieved using piezoelectric actuation of air bubbles trapped inside the chamber.

11. Summary

The present trend in miniaturized bio-chip devices looks promising to fulfil the target for clinical practices. Development of microchannel fluidics enabled integration of multi-components in a single chip. There is a need to replace silicon technology with newer materials such as polymer and elastomer for micro devices for reasons such as ease of batch fabrication, cost, electrically insulation and optically transparency. It is necessary that DNA amplification be coupled to sample preparation steps and post PCR detection to establish a completely automated LOC device. While several groups have demonstrated laboratory prototypes with one or more functions integrated on a single chip, it is clear that several challenges have to be overcome before commercial systems become widely available.

Acknowledgements

The authors thank Mrs. Baishali Chatterjee for PDMS device fabrication, Dr. Debjani Paul for the induction heater and Prof. Vasant Natarajan for the fluorescence setup. This work was partially supported by BRNS, Department of Atomic Energy and the Life Sciences Research Board (LSRB) of the Government of India. The PDMS work was supported by the "Centre of excellence in Nanoelectronics at IISc" funded by MCIT, Government of India.

Received 27 June 2007; revised 20 August 2007.

References

1. L.J. Kricka and P. Wilding. Microchip PCR. *Anal. Bioanal. Chem.*, **377**: 820–825, 2003.
2. E.T. Lagally, J.R. Scherer, R.G. Blazej, N.M. Toriello, B.A. Diep, M. Ramchandrani, G.F. Sensabaugh, L.W. Riley, and R.A. Mathies. Integrated portable genetic analysis microsystem for pathogen/infectious disease detection. *Anal. Chem.*, **76**, 3162–3170, 2004.
3. P.A. Auroux, Y. Koc, A. deMello, A. Manz, and P.J.R. Day. Miniaturised nucleic acid analysis. *Lab Chip*, **4**, 534–546, 2004.
4. C. Zhang, J. Xu, W. Ma, and W. Zheng. PCR microfluidic devices for DNA amplification. *Biotechnol. Adv.*, **24**, 243–284, 2006.
5. K.B. Mullis. The unusual origin of the polymerase chain reaction. *Sci. Am.*, **262**, 36–43, 1990.
6. R.K. Saiki, S. Scharf, F. Faloona, K.B. Mullis, G.T. Horn, H.A. Erlich, and N. Arnheim. Enzymatic amplification of β-globin genomic sequences and restriction site analysis for diagnosis of sickle cell anemia. *Science*, **230**, 1350–1354, 1985.
7. C.T. Wittwer, G.C. Fillmore, and D.J. Garling. Minimizing the time required for DNA amplification by efficient heat transfer to small samples. *Anal. Biochem.*, **186**, 328–331, 1990.
8. M.A. Northrup, M.T. Ching, R.M. White, and R.T. Watson. DNA amplification with a microfabricated reaction chamber. In *Transducers'93, seventh international conference on solid state Sens Actuators, Yokahama, Japan*, pages 924–926, 1993.
9. P. Neuzil, J. Pipper, and T.M. Hsieh. Disposable real-time microPCR device: lab-on-a-chip at a low cost. *Mol. Biosyst.*, **2**, 292–298, 2006.
10. A.T. Woolley, D. Hadley, P. Landre, A.J. deMellow, R.A. Mathies, and M.A. Northrup. Functional integration of PCR amplification and capillary electrophoresis in a microfabricated DNA analysis device. *Anal. Chem.*, **68**, 4081–4086, 1996.
11. J.H. Daniel, S. Iqbal, R.B. Millington, D.F. Moore, C.R. Lowe, D.L. Leslie, M.A. Lee, and M.J. Pearce. Silicon microchambers for DNA amplification. *Sens. Actuators A*, **71**, 81–88, 1998.
12. Y.C. Lin, C.C. Yang, and M.Y. Huang. Simulation and experimental validation of micro polymerase chain reaction chips. *Sens. Actuators B*, **71**, 127–133, 2000.
13. D.S. Yoon, Y.S. Lee, Y. Lee, H.J. Cho, S.W. Sung, K.W. Oh, J. Cha, and G. Lim. Precise temperature control and rapid thermal cycling in a micromachined DNA polymerase chain reaction chip. *J. Micromech. Microeng.*, **12**, 813–823, 2002.
14. Q. Zou, Y. Miao, Y. Chen, U. Sridhar, C.S. Chong, T. Chai, Y. Tie, C.H.L. Teh, T.M. Lim, and C.K. Heng. Micro-assembled multi-chamber thermal cycler for low-cost reaction chip thermal multiplexing. *Sens. Actuators A*, **102**, 114–121, 2002.
15. Y.S. Shin, K. Cho, S.H. Lim, S. Chung, S.J. Park, C. Chung, D.C. Han, and J.K. Chang. PDMS-based micro PCR chip with Parylene coating. *J. Micromech. Microeng.*, **13**, 768–774, 2003.
16. J.E. Ali, I.R.P. Nielsen, C.R. Poulsen, D.D. Bang, P.Telleman, and A. Wolff. Simulation and experimental validation of a SU-8 based PCR thermocycler chip with integrated heaters and temperature sensor. *Sens. Actuators A*, **110**, 3–10, 2004.
17. Z.Q. Zou, X. Chen, Q.H. Jin, M.S. Yang, and J.L. Zhao. A novel miniaturized PCR multi-reactor array fabricated using flip-chip bonding techniques. *J. Micromech. Microeng.*, **15**, 1476–1481, 2005.
18. C. Ke, A.M. Kelleher, H. Berney, M. Sheehan, and A. Mathewson. Single step cell lysis/PCR detection of *Escherichia coli* in an independently controllable silicon microreactor. *Sens. Actuators B*, **120**, 538–544, 2007.
19. Y.K. Cho, J. Kim, Y. Lee, Y.A. Kim, K. Namkoong, H. Lim, K.W. Oh, S. Kim, J. Han, C. Park, Y.E. Pak, C.S. Ki, J.R. Choi, H.K. Myeong, and C. Ko. Clinical evaluation of micro-scale chip-based PCR system for rapid detection of hepatitis B virus. *Biosens. Bioelectron.*, **21**, 2161–2169, 2006.
20. Z.Q. Niu, W.Y. Chen, S.Y. Shao, X.Y. Jia, and W.P. Zhang. DNA amplification on a PDMS-glass hybrid microchip. *J. Micromech. Microeng.*, **16**, 425–433, 2006.
21. J. Xiaoyu, N. Zhiqiang, C. Wenyuan, and Z. Weiping. Polydimethylsiloxane (PDMS)-based spiral channel PCR chip. *Electron. Lett.*, 41:no. 16, 2005.

22. M.U. Kopp, A.J. deMello, and A. Manz. Chemical amplification: continuous-flow PCR on a chip. *Science*, **280**, 1046–1048, 1998.
23. Y. Zhang, D.J. Isaacman, R.M. Wadowsky, J.R. White, J.C. Post, and G.D. Ehrlich. Detection of *Streptococcus pneumoniae* in whole blood by PCR. *J. Clin. Microbiol.*, **33**, 596–601, 1995.
24. R. Higuchi, C.H.V. Beroldingen, G.F. Sensabaugh, and H.A. Erlich. DNA typing from single hairs. *Nature*, **332**, 543–546, 1988.
25. S.A. Ansari, S.R. Farrah, and G.R. Chaudhry. Presence of human immunodeficiency virus nucleic acids in wastewater and their detection by polymerase chain reaction. *Appl. Environ. Microbiol.*, **58**, 3984–3990, 1992.
26. S.Y. Lee, J. Bollinger, D. Bezdicek, and A. Ogram. Estimation of the abundance of an uncultured soil bacterial strain by a competitive quantitative PCR method. *Appl. Environ. Microbiol.*, **62**, 3787–3793, 1996.
27. C.T. Wittwer, G.C. Fillmore, and D.R. Hillyard. Automated polymerase chain reaction in capillary tubes with hot air. *Nucleic Acids Res.*, **17**, 4353–4357, 1989.
28. A.F.R. Hühmer and J.P. Landers. Noncontact infrared-mediated thermocycling for effective polymerase chain reaction amplification of DNA in nanoliter volumes. *Anal. Chem.*, **72**, 5507–5512, 2000.
29. B.C. Giordano, J. Ferrance, S. Swedberg, A.F.R. Hühmer, and J.P. Landers. Polymerase chain reaction in polymeric microchips: DNA amplification in less than 240 seconds. *Anal. Biochem.*, **291**, 124–132, 2001.
30. J. Liu, M. Enzelberger, and S. Quake. A nanoliter rotary device for polymerase chain reaction. *Electrophoresis*, **23**, 1531–1536, 2002.
31. N.J. Panaro, X.J. Lou, P. Fortina, L.J. Kricka, and P. Wilding. Surface effects on PCR reactions in multichip microfluidic platforms. *Biomed. Microdevices*, **6**, 75–80, 2004.
32. M.J. Madou. *Fundamentals of microfabrication*. CRC Press, 1997.
33. J.E. Mark. *Polymer data handbook*. Oxford Univ. Press, 1999.
34. M.A. Shoffner, J. Cheng, G.E. Hvichia, L.J. Kricka, and P. Wilding. Chip PCR.I. Surface passivation of microfabricated silicon-glass chips for PCR. *Nucleic Acids Res.*, **24**, 375–379, 1996.
35. R.P. Oda, M.A. Strausbauch, A.F.R. Hühmer, N. Borson, S.R. Jurrens, J. Craighead, P.J. Wettstein, B. Eckloff, B. Kline, and J.P. Landers. Infrared-mediated thermocycling for ultrafast polymerase chain reaction amplification of DNA. *Anal. Chem.*, **70**, 4361–4368, 1998.
36. I. Erill, S. Campoy, J. Rus, L. Fonseca, A. Ivorra, Z. Navarro, J.A. Plaza, J. Aguiló, and J. Barbé. Development of a CMOS-compatible PCR chip: comparison of design and system strategies. *J. Micromech. Microeng.*, **14**, 1558–1568, 2004.
37. R.C. Anderson, X. Su, G.J. Bogdan, and J. Fenton. A miniature integrated device for automated multistep genetic assays. *Nucleic Acids Res.*, 28:e60, 2000.
38. I. Schneegaß, R. Bräutigam, and J.M. Köhler. Miniaturized flow-through PCR with different template types in a silicon chip thermocycler. *Lab Chip*, **1**, 42–49, 2001.
39. T.B. Taylor, E.S.W. Deen, E. Picozza, T.M. Woudenberg, and M. Albin. Optimization of the performance of the polymerase chain reaction in silicon-based microstructures. *Nucleic Acids Res.*, **25**, 3164–3168, 1997.
40. I. Erill, S. Campoy, N. Erill, J. Barbé, and J. Aguiló. Biochemical analysis and optimization of inhibition and adsorption phenomena in glass-silicon PCR-chips. *Sens. Actuators B*, **96**, 685–692, 2003.
41. D.B. Lee. Anisotropic etching of silicon. *J. Appl. Phys.*, **40**, 4569–4574, 1969.
42. K.E. Bean. Anisotropic etching of silicon. *IEEE Trans. Electron. Devices*, ED-**25**, 1185–1193, 1978.
43. Y. Xia and G. M. Whitesides. Soft lithography. *Annu. Rev. Mater. Sci.*, **28**, 153–184, 1998.
44. J.C. McDonald, D.C. Duffy, J.R. Anderson, D.T. Chiu, H. Wu, O.J.A. Schueller, and G.M. Whitesides. Fabrication of microfluidic systems in poly(dimethylsiloxane). *Electrophoresis*, **21**, 27–40, 2000.
45. J.C. McDonald and G.M. Whitesides. Poly(dimethylsiloxane) as a material for fabricating microfluidic devices. *Acc. Chem. Res.*, **35**, 491–499, 2002.
46. G.S. Fiorini and D.T. Chiu. Disposable microfluidic devices: fabrication, function, and application. *BioTechniques*, **38**, 429–446, 2005.
47. C. Yamahata, F. Lacharme, and M.A.M. Gijs. Glass valveless micropump using electromagnetic actuation. *Microelectron. Eng.*, **78–79**, 132–137, 2005.
48. C.W. Li, C.N. Cheung, J. Yang, C.H. Tzang, and M. Yang. PDMS-based microfluidic device with multi-height structures fabricated by single-step photolithography using printed circuit board as masters. *Analyst*, **128**, 1137–1142, 2003.
49. A.P. Sudarsan and V.M. Ugaz. Printed circuit technology for fabrication of plastic-based microfluidic devices. *Anal. Chem.*, **76**, 3229–3235, 2004.
50. D.C. Duffy, J.C. McDonald, O.J.A. Schueller, and G.M. Whitesides. Rapid prototyping of microfluidic systems in poly(dimethylsiloxane). *Anal. Chem.*, **70**, 4974–4984, 1998.
51. Q. Xiang, B. Xu, R. Fu, and D. Li. Real time PCR on disposable PDMS chip with a miniaturized thermal cycler. *Biomed. Microdevices*, **7**, 273–279, 2005.
52. S. Li and S. Chen. Polydimethylsioxane fluidic interconnects for microfluidic systems. *IEEE Trans. Adv. Pack.*, **26**, 242–247, 2003.
53. M.A. Unger, H.P. Chou, T. Thorsen, A. Scherer, and S.R. Quake. Monolithic microfabricated valves and pumps by multilayer soft lithography. *Science*, **288**, 113–116, 2000.
54. J.R. Anderson, D.T. Chiu, R.J. Jackman, O. Cherniavskaya, J.C. McDonald, H. Wu, S.H. Whitesides, and G.M. Whitesides. Fabrication of topologically complex three-dimensional microfluidic systems in PDMS by rapid prototyping. *Anal. Chem.*, **72**, 3158–3164, 2000.
55. S. Poser, T. Schulz, U. Dillner, V. Baier, J.M. Köhler, D. Schimkat, G. Mayer, and A. Siebert. Chip elements for fast thermocycling. *Sens. Actuators A*, **62**, 672–675, 1997.
56. Z. Zhao, Z. Cui, D. Cui, and S. Xia. Monolithically integrated PCR biochip for DNA amplification. *Sens. Actuators A*, **108**, 162–167, 2003.
57. K. Sun, A. Yamaguchi, Y. Ishida, S. Matsuo, and H. Misawa. A heater-integrated transparent microchannel chip for continuous-flow PCR. *Sens. Actuators B*, **84**, 283–289, 2002.
58. Y.C. Lin, M.Y. Huang, K.C. Young, T.T. Chang, and C.Y. Wu. A rapid micro-polymerase chain reaction system for hepatitis C virus amplification. *Sens. Actuators B*, **71**, 2–8, 2000.
59. J. Khandurina, T.E. McKnight, S.C. Jacobson, L.C. Waters, R.S. Foote, and J.M. Ramsey. Integrated system for rapid PCR-based DNA analysis in microfluidic devices. *Anal. Chem.*, **72**, 2995–3000, 2000.
60. M. Krishnan, V.M. Ugaz, and M.A. Burns. PCR in a Rayleigh-Bérnard convection cell. *Science*, **298**, 793, 2002.
61. D. Braun, N.L. Goddard, and A. Libchaber. Exponential DNA replication by laminar convection. *Phys. Rev. Lett.*, **91**, 158103, 2003.
62. D.M. Heap, M.G. Herrmann, and C.T. Wittwer. PCR amplification using electrolytic resistance for heating and temperature monitoring. *BioTechniques*, **29**, 1006–1012, 2000.

63. D.S. Lee, M.H. Wu, U. Ramesh, C.W. Lin, T.M. Lee, and P.H. Chen. A novel real-time PCR machine with a miniature spectrometer for fluorescence sensing in a micro liter volume glass capillary. *Sens. Actuators B*, **100**, 401–410, 2004.
64. Y. Tanaka, M.N. Slyadnev, A. Hibara, M. Tokeshi, and T. Kitamori. Non-contact photothermal control of enzyme reactions on a microchip by using a compact diode laser. *J. Chromatogr. A*, **894**, 45–51, 2000.
65. M.N. Slyadnev, Y. Tanaka, M. Tokeshi, and T. Kitamori. Photothermal temperature control of a chemical reaction on a microchip using an infrared diode laser. *Anal. Chem.*, **73**, 4037–4044, 2001.
66. D. Pal and V. Venkataraman. A portable battery-operated chip thermocycler based on induction heating. *Sens. Actuators A*, **102**, 151–156, 2002.
67. C.R. Smith, D.R. Sabatino, and T.J. Praisner. Temperature sensing with thermochromic liquid crystals. *Exp. Fluids*, **30**, 190–201, 2001.
68. J. Noh, S.W. Sung, M.K. Jeon, S.H. Kim, L.P. Lee, and S.I. Woo. In situ thermal diagnostics of the micro-PCR system using liquid crystals. *Sens. Actuators A*, **122**, 196–202, 2005.
69. A.M. Chaudhari, T.M. Woudenberg, M. Albin, and K.E. Goodson. Transient liquid crystal thermometry of microfabricated PCR vessel arrays. *J. Microelectromech. Syst.*, **7**, 345–355, 1998.
70. D. Ross, M. Gaitan, and L.E. Locascio. Temperature measurement in microfluidic systems using a temperature-dependent fluorescent dye. *Anal. Chem.*, **73**, 4117–4123, 2001.
71. S. Mondal and V. Venkataraman. Novel fluorescence detection technique for non-contact temperature sensing in microchip PCR. *J. Biochem. Biophys. Methods*, **70**, 773–777, 2007.
72. K.L. Davis, K.L.K. Liu, M. Lanan, and M.D. Morris. Spatially resolved temperature measurements in electrophoresis capillaries by Raman thermometry. *Anal. Chem.*, **65**, 293–298, 1993.
73. S.H. Kim, J. Noh, M.K. Jeon, K.W. Kim, L.P. Lee, and S.I. Woo. Micro-Raman thermometry for measuring the temperature distribution inside the microchannel of a polymerase chain reaction chip. *J. Micromech. Microeng.*, **16**, 526–530, 2006.
74. M.E. Lacey, A.G. Webb, and J.V. Sweedler. Monitoring temperature changes in capillary electrophoresis with nanoliter-volume NMR thermometry. *Anal. Chem.*, **72**, 4991–4998, 2000.
75. S. Jeon, J. Turner, and S. Granick. Noncontact temperature measurement in microliter-sized volumes using fluorescent-labeled DNA oligomers. *J. Am. Chem. Soc.*, **125**, 9908–9909, 2003.
76. H. Zipper, H. Brunner, J. Bernhagen, and F. Vitzthum. Investigations on DNA intercalation and surface binding by SYBR green I, its structure determination and methodological implications. *Nucleic Acids Res.*, 32:e103, 2004.
77. R. Higuchi, G. Dollinger, P.S. Walsh, and R. Griffith. Simultaneous amplification and detection of specific DNA sequences. *Bio/Technology*, **10**, 413–417, 1992.
78. R. Higuchi, C. Fockler, G. Dollinger, and R. Watson. Kinetic PCR analysis: real-time monitoring of DNA amplification reactions. *Bio/technology*, **11**, 1026–1030, 1993.
79. W. Liu and D.A. Saint. Validation of a quantitative method for real time PCR kinetics. *Biochem. Biophys. Res. Commun.*, **294**, 347–353, 2002.
80. B. Arezi, W. Xing, J.A. Sorge, and H.H. Hogrefe. Amplification efficiency of thermostable DNA polymerases. *Anal. Biochem.*, **321**, 226–235, 2003.
81. C.T. Wittwer, M.G. Herrmann, A.A. Moss, and R.P. Rasmussen. Continuous fluorescence monitoring of rapid cycle DNA amplification. *BioTechniques*, **22**, 130–138, 1997.
82. C.T. Wittwer, K.M. Ririe, R.V. Andrew, D.A. David, R.A. Gundry, and U.J. Balis. The lightcycler: a microvolume multisample fluorimeter with rapid temperature control. *BioTechniques*, **22**, 176–181, 1997.
83. T.B. Morrison, J.J. Weis, and C.T. Wittwer. Quantification of low-copy transcripts by continuous SYBR green I monitoring during amplification. *BioTechniques*, **24**, 954–962, 1998.
84. P. Belgrader, S. Young, B. Yuan, M. Primeau, L.A. Christel, F. Pourahmadi, and M.A. Northrup. A battery-powered notebook thermal cycler for rapid multiplex real-time PCR analysis. *Anal. Chem.*, **73**, 286–289, 2001.
85. Y.C. Lin, M. Li, M.T. Chung, C.Y. Wu, and K.C. Young. Real-time microchip polymerase-chain-reaction system. *Sens. Mater.*, **14**, 199–208, 2002.
86. A. Gulliksen, L. Solli, F. Karlsen, H. Rogne, E. Hovig, T. Nordstrϕm, and R. Sirev$\mathring{a}$g. Real-time nucleic acid sequence-based amplification in nanoliter volumes. *Anal. Chem.*, **76**, 9–14, 2004.
87. L. Novak, P. Neuzil, J. Pipper, Y. Zhang, and S. Lee. An integrated fluorescence detection system for lab-on-a-chip applications. *Lab Chip*, **7**, 27–29, 2007.
88. J.R. Webster, M.A. Burns, D.T. Burke, and C.H. Mastrangelo. Monolithic capillary electrophoresis device with integrated fluorescence detector. *Anal. Chem.*, **73**, 1622–1626, 2001.
89. J.A. Higgins, S. Nasarabadi, J.S. Karns, D.R. Shelton, M. Cooper, A. Gbakima, and R.P. Koopman. A handheld real time thermal cycler for bacterial pathogen detection. *Biosens. Bioelectron.*, **18**, 1115–1123, 2003.
90. C.T. Wittwer and D.J. Garling. Rapid cycle DNA amplification: time and temperature optimization. *BioTechniques*, **10**, 76–83, 1991.
91. T. Ederhof, N.G. Walter, and A. Schober. On-line polymerase chain reaction (PCR) monitoring. *J. Biochem. Biophys. Methods*, **37**, 99–104, 1998.
92. S. Mondal and V. Venkataraman. In situ monitoring of polymerase extension rate and adaptive feedback control of PCR by using fluorescence measurements. *J. Biochem. Biophys. Methods*, **65**, 97–105, 2005.
93. N.C. Cady, S. Stelick, M.V. Kunnavakkam, and C.A. Batt. Real-time PCR detection of *Listeria monocytogenes* using an integrated microfluidics platform. *Sens. Actuators B*, **107**, 332–341, 2005.
94. S. Mondal, D. Paul, and V. Venkataraman. Dynamic optimization of on-chip polymerase chain reaction by monitoring intracycle fluorescence using fast synchronous detection. *Appl. Phys. Lett.*, **90**, 013902, 2007.
95. K.M. Ririe, R.P. Rasmussen, and C.T. Wittwer. Product differentiation by analysis of DNA melting curves during the polymerase chain reaction. *Anal. Biochem.*, **245**, 154–160, 1997.
96. S. Giglio, P.T. Monis, and C.P. Saint. Demonstration of preferential binding of SYBR green I to specific DNA freagments in real-time multiplex PCR. *Nucleic Acids Res.*, 31:e136, 2003.
97. W. Li, B. Xi, W. Yang, M. Hawkins, and U.K. Schubart. Complex DNA melting profiles of small PCR products revealed using SYBR green I. *BioTechniques*, **35**, 702–706, 2003.
98. A. Karsai, S. M$\ddot{u}$ller, S. Platz, and M.T. Hauser. Evaluation of a home made SYBR green I reaction mixture for real-time PCR quantification of gene expression. *BioTechniques*, **32**, 790–796, 2002.
99. B.C. Millar, X. Jiru, J.E. Moore, and J.A.P. Earle. A simple and sensitive method to extract bacterial, yeast and fungal DNA from blood culture material. *J. Microbiol. Methods*, **42**, 139–147, 2000.
100. M.C. Breadmore, K.A. Wolfe, I.G. Arcibal, W.K. Leung, D. Dickson, B.C. Giordano, M.E. Power, J.P. Ferrance, S.H. Feldman, P.M. Norris, and J.P. Landers. Microchip-based purification of DNA from biological samples. *Anal. Chem.*, **75**, 1880–1886, 2003.

101. P. Wilding, L.J. Kricka, J. Cheng, G. Hvichia, M.A. Shoffner, and P. Fortina. Integrated cell isolation and polymerase chain reaction analysis using silicon microfilter chambers. *Anal. Biochem.*, **257**, 95–100, 1998.
102. P.K. Yuen, L.J. Kricka, P. Fortina, N.J. Panaro, T. Sakazume, and P. Wilding. Microchip module for blood sample preparation and nucleic acid amplification reactions. *Genome Res.*, **11**, 405–412, 2001.
103. N.C. Cady, S. Stelick, and C.A. Batt. Nucleic acid purification using microfabricated silicon structures. *Biosens. Bioelectron.*, **19**, 59–66, 2003.
104. N. Zhang, H. Tan, and E.S. Yeung. Automated and integrated system for high-throughput DNA genotyping directly from blood. *Anal. Chem.*, **71**, 1138–1145, 1999.
105. M. Hashimoto, Y. He, and E.S. Yeung. On-line integration of PCR and cycle sequencing in capillaries: from human genomic DNA directly to called bases. *Nucleic Acids Res.*, 31:e41, 2003.
106. C.Y. Lee, G.B. Lee, J.L. Lin, F.C. Huang, and C.S. Liao. Integrated microfluidic systems for cell lysis, mixing/pumping and DNA amplification. *J. Micromech. Microeng.*, **15**, 1215–1223, 2005.
107. R.H. Liu, J. Yang, R. Lenigk, J. Bonanno, and P. Grodzinski. Self-contained, fully integrated biochip for sample preparation, polymerase chain reaction amplification, and DNA microarray detection. *Anal. Chem.*, **76**, 1824–1831, 2004.

V. Venkataraman completed his B.Tech in 1988 and his Ph.D. in 1994. He joined the faculty of the Indian Institute of Science in 1994 where he is currently an Associate Professor. His primary area of interest is Semiconductor Physics and Technology, especially electrical and transport properties of semiconductor heterostructures. Over the last five years, he has also been involved with applications of semiconductor technology to BioMEMS devices, especially PCR microdevices. He has published about 30 papers in international journals.

Sudip Mondal is a PhD student of Department of Physics at Indian Institute of Science (IISc) working with Prof. V. Venkataraman. His area of research includes development of PCR devices and fluorescence based detection. He has received his Masters degree in Physics from Indian Institute of Science, Bangalore, India in 2004. He has completed his bachelor degree in Physics from St. Xaviers College under Calcutta University in 2001.